Aerodynamic Study Of Tall Buildings Under Wind Load

A REPORT

SUBMITTED IN PARTIAL FULFILLMENT OF THE
REQUIREMENTS FOR THE AWARD OF THE DEGREE
OF

MASTER OF
TECHNOLOGY IN

CIVIL ENGINEERING

Submitted By

HEMANT GAUTAM

(2K19/STE/12)

UNDER THE SUPERVISION OF

DR. RITU RAJ

CIVIL ENGINEERING DEPARTMENT

DELHI TECHNOLOGICAL UNIVERSITY

(Formerly Delhi College of Engineering)

Bawana Road, Delhi-110042

July, 2021

CANDIDATE DECLARATION

I, "**Hemant Gautam"** student of M. Tech Structural Engineering, DTU hereby declare that the project dissertation titled **"Aerodynamic Study of Tall Buildings under Wind Load"** is submitted to the Department of Civil Engineering, Delhi Technological University, Delhi in partial fulfilment of the requirement for the award of the degree of Master of Technology, is original and not copied from any source without proper citation. This work has never before been used to give a degree, diploma, associateship, fellowship, or other equivalent title or recognition.

Place: Delhi

Hemant Gautam

(2K19/STE/12)

CIVIL ENGINEERING DEPARTMENT

DELHI TECHNOLOGICAL UNIVERSITY

(Formerly Delhi College of Engineering)

Bawana Road Delhi-110042

CERTIFICATE

I hereby certify that the Project Dissertation titled "Aerodynamic Study of Tall Buildings Under Wind Load" which is submitted by Hemant Gautam 2K19/STE/12) Civil Engineering Department, Delhi Technological University, Delhi in partial fulfilment of the requirement for the award of the degree of Master of Technology, is a record of the project work carried out by the student under my supervision. To the best of my knowledge, this work has never before been submitted to give a degree, diploma, associateship, fellowship, or other equivalent title or recognition.

Place: Delhi

Dr. RITU RAJ

Supervisor

Assistant Professor

Department of Civil Engineering

Delhi Technological University

Signature: 

Date:30.07.2021

ACKNOWLEDGEMENT

I would like to express my gratitude to my mentor, Dr. RITURAJ who gave me the opportunity to carry out this wonderful project on the topic "Aerodynamic Study of Tall Buildings Under Wind Load" which helped me in boosting my technical knowledge and experimental skills. His directions and support were the basic essence of motivation for me.

I feel of paucity of words to express our thanks to the honourable Head of Department of Civil Engineering, Dr. V.K Minocha, for allowing me to utilize the department facilities and have been a constant source of motivation during the course of project.

I express my deepest sense of gratitude towards the Professors of Civil Engineering Department who helped me in formulating the problem statement and clarifying our doubts regarding the learning about the tall buildings.

At last, I would like to thank to PhD scholar Rahul Kumar Meena and my colleagues who helped me by actively participating in discussions and giving their valuable feedbacks. Their presence and support were invaluable. Finally, we would like to thank our parents for their undying support, motivation and providing me the golden opportunity to study in this prestigious institution.

Signature: 

Name: HEMANT GAUTAM

Roll No.: 2K19/STE/12

Date: 30.07.2021

Table of Contents

List of Tables

List of Figures

1 Introduction

1.1 Overview

With the advancement of technology and enormous growth in population, the need and design of tall structures with different configuration has been a growing trend. High rise structures have always fascinated from the beginning of civilization and are unique in various aspects such as consideration of lateral deflections. High Rise Buildings are cantilever structures subjected to substantial lateral loads and responses. In design of such structures for wind loading, occupant comfort along with serviceability is the dominant criteria along with safety of structure.

Wind is a complicated phenomenon in which motion of an individual particle is so unpredictable that one need to be concerned about statistical distribution of velocity rather than just simple averages. The total wind force is equal to the sum of windward pressure and leeward suction, although each has its own local effect.

In tall buildings, the aerodynamic and dynamic effects are to be analyzed along with the static effects, whereas in low rise buildings only static effects are sufficient to be considered. Such structures are subjected to along with as well as across wind effects. The along wind effect are caused primarily due to buffeting phenomenon caused due to gust effects whereas across wind induced effects are due to vortex shedding. Galloping phenomenon are more susceptible to structural elements that are not circular, which is due to transverse oscillations of structures due to wind forces that are in phase with motion. Flutter is another unstable oscillatory motion.

Eddies of varied sizes and rotating properties make up wind. Wind is turbulent or gusty because of these eddies. Strong winds' gustiness is mostly caused by interaction with surface characteristics at lower altitudes of the atmosphere. The average wind speed during a ten-minute or longer period of time tends to rise with height, while the gustiness tends to reduce with height. However, the most common design that is proposed for tall structures are rectangular or square shaped buildings. The design of tall buildings subjected to wind loads does require a deeper grasp of mechanism of loads.

In order to understand the aerodynamics and to anticipate its behavior precisely isn’t an easy task to do. Wind responses on a building is dynamic in nature due to its gusty nature or turbulence and is influenced by various factors such as roughness, terrain type, the shape, and

the surrounding buildings. Therefore, motion of wind is turbulent in nature causing particles of air to move randomly in atmosphere. Wind Pressure on a high-rise building depends upon wind velocity, the surface and plan of structure of building, interference effect from the surrounding natural or man-made structures. The dynamic wind leads to impart phenomena such as buffeting by vortices and turbulence shed by gusts and structures respectively, buffeting caused due to wake region from another structure, and aerodynamic damping.

The total wind force is equal to the sum of windward pressure and leeward suction, although each has its own local effect. The designers consult appropriate wind load standards such as (AS/NZS 1170.2:2011), (ASCE 7-10: Minimum Design Loads for Buildings and Other Structures), (BS 6399-2:1997 - Loading for Buildings. Code of Practice for Wind Loads (British Standard)), (EN 1991-1-4: Eurocode 1: Actions on Structures - Part 1-4: General Actions - Wind Actions, 2010), (IS 875.3: Code of Practice for Design Loads (Other than Earthquake) for Buildings and Structures - Part 3 : Wind Loads (IS 875 : Part 3) to estimate the design pressure coefficients and force coefficients for such buildings subjected to wind induced loads. These standards, on the other hand, gives information for simple cross-sectional shapes with a small number of wind incidence angles. These codes do not include information on wind loadings for buildings with unusual forms. As a result, wind tunnel testing on models of such structures is popular. Similarly, there isn't much guidance on how to think about interference effects, a building cannot be considered independent of its surroundings when designing for wind loads. The impact of neighboring structures and land configuration is significant, and hence must be taken into account.

1.2 Loads Acting on a Structure

Dead loads, live loads, earthquake loads, snow loads, and wind loads are all kinds of loads acting on a structure. A structure's safety is assessed in relation to all possible load combinations.

The following subcategories can be used to classify loads acting on a structure:

a) Geophysical Forces
b) Human made Forces

Geophysical forces, which include gravitational, meteorological, and seismological forces, are caused by continuous changes in nature. Human-made forces are the result of people and equipment moving around, as well as fluctuations in shocks caused by machines, tools, blasts, and impact. Geophysical and human-made forces, on the other hand, are generally interdependent.

Loads are also classified as:

a) Static load
b) Dynamic load

Static loads are permanent part of structure and don’t change with time and space within a structure whereas dynamic load on the other hand, are temporary in nature and are a function of space within a structure.

The wind load is dynamic in nature. This means that its magnitude fluctuates with respect to time and space. As a result, analysing and modelling such a load and its relative impacts on a structure may be fairly difficult and involve a lot of math, computational fluid dynamics, and structural analysis understanding.

1.3 About CFD

CFD (Computation Fluid Dynamics) is the branch of fluid dynamics that analyse and solve the fluid flow problems using numerical approach and data structures. In aerodynamics and hydrodynamics, where lift and drag, as well as pressure and velocities, are parameters, CFD analysis are widely employed. CFD analysis saves time in the design process and are hence cheaper and less time consuming compared to conventional testing.

In CFD, all the required parameters can be analysed and measured at once with a high resolution of time and space. Since CFD analysis approximates a real physical solution, therefore it cannot exclude physical testing procedure completely.

CFD Analysis includes following phases: -

1. PRE-PROCESSING
2. SOLVING
3. POST PROCESSING

Wind Tunnel Testing is widely recognized in the scientific and engineering community. Wind tunnel results have demonstrated to be representative of real-world scenarios when the modelling appropriately accounts for the features of the atmosphere and exact scaling is done. Wind tunnel testing provides information about the dependence of particular response of wind velocity.

CFD has the following advantages over wind tunnel testing:

- Comprehensive domain analysis
- Simple alternative analysis
- Improved visualisation of outcomes
- Cost-effective
- In a wind tunnel, measuring wind direction, pollutant concentrations, chemical reactions, radiation, and so on is difficult. In general, CFD is more adaptable when it comes to accounting for the specific elements of each project.

1.4 Need of study

Simple cross-sectional shapes with limited wind incidence angles are covered by codal standards. These codes do not include information on wind loadings for buildings with unconventional geometries. On the other hand, the use of CFD for determining wind responses is becoming immensely popular. CFD has expanded as a tool to replace wind tunnel testing as it is quicker, less expansive and give more information and control to designers.

1.5 Objective and Scope

- To investigate the mean wind pressure coefficient on different faces of building using CFD technique.
- To compare the mean pressure coefficients of the models for isolated condition with the results given in codes for 0° and 90°.
- To plot pressure contours for different faces of building considering different angle of attack.
- To find out Cp with different angle of attacks and to plot results graphically to interpret the scope of side ratio effect.

1.6 Limitation of CFD

- Error may be introduced due to simple flow models or simplified boundary condition.
- Computations time for evaluation may extend for larger models with unconventional shapes for finer mesh solutions.
- CFD tools provide quicker simulation, but they are black boxes, and the user has no way of knowing whether the correct boundary condition is used.
- These models generate massive amounts of data and outputs, and possible flaws are readily ignored, especially if the model is large and complicated, due to increased processing power and more powerful software.
- Due to a lack of understanding of structural behaviors and modelling, it is all too simple to accept the conclusions without question. Furthermore, differing modelling approaches have a significant impact on force and stress distribution.
- This can lead to lengthy discussions and conflicts between engineers, as different calculations on the same building typically provide different findings.

2 Literature Review

2.1 General

Since the 1960s, several researchers have derived a wealth of useful information by assuming that wind pressure behaves in a static manner. This method assisted in estimating the results of wind tunnel tests at a uniform steady velocity.

The history of tall structure design is enormous by itself. Architects and structural engineers collaborated for generations to create taller buildings. Skyscrapers of today are the consequence of constant exploration, invention, and discovery. Urbanization in the twentieth and twenty-first centuries stimulated the development of tall buildings, which became taller and taller as demand increased. Prior to the nineteenth century, the world's tallest structure was a church. In the nineteenth century, Chicago pioneered a new type of structure that relied on iron or steel to support the weight of the structure. The Home Insurance Building in Chicago, which stands 42 metres tall, was the world's first skyscraper in 1885. Following that, an increasing number of tall buildings were constructed, including the Empire State Building (102 stories) in 1931. Following that, with the rapid advancement of construction technology and the development of computer modelling techniques, a rising number of tall buildings were constructed all over the world.

Cross sections should be carefully chosen as the building grows taller, keeping in mind the demand for serviceability and functioning, as new lateral forces are created from unintended deflections. In most cases, wind load is the governing load in tall building design for lateral stability system design, as opposed to seismic loading. This is owing to the tall building's longer natural period, which results in a smaller earthquake response than a low-rise building. However, depending on the location and significance of the structure, a necessary check may be required.

2.2 Codal Provision

2.2.1 British Standard (IIS EN 199h14, 2005)

For each of the load conditions under consideration, this code of practise provides guidelines on determining natural wind activities for structural design of buildings and civil engineering works. This code of practise applies to buildings and structures up to 200 metres in height, as well as bridges with a span of no more than 200 metres. This code also intends to forecast typical wind behaviours on land-based constructions and their components. For irregular cross-sectional shapes, there is no information on wind pressure distribution. This rule of practise also excludes information on different skew angles of wind.

2.2.2 American Standard (ASCE4, 2002)

ASCE-7 provides thorough information on wind loads on low-rise buildings with various roof types. This standard also includes information on low-rise buildings with various aspect ratios. However, there is a scarcity of data on wind loads on high-rise structures with various cross-sectional shapes. In the case of skew wind, no information is accessible either.

2.2.3 Australia and New Zealand Standard (AS/NZS-1 170-2, 2011)

This code of practise applies to structures that meet the following criteria: I height of less than or equal to 200 metres, and (ii) roof span of less than 100 metres. Wind loads on structures other than offshore structures, such as bridges and transmission towers, are also included in this code. This code of practise does not include information regarding cross-sectional shapes other than square and rectangular. When a building is hit by a skew wind angle, there is very little information regarding the pressure distribution.

2.2.4 Indian Standard (875, part-3, 1987)

According to IS: 875 (Part-3), deals with wind loads to be considered when designing buildings, structures and components thereof. In this code, a single wind map is provided in this code, with the basic maximum wind speed in m/s (peak gust speed averaged over a short time interval of about 3 seconds duration). Based on the most recent wind data, the wind speeds were calculated over a 50-year return period. Modification parameters were incorporated to adjust the fundamental wind speed to account for geography, local topography, structure size, and other factors. For a wide range of clad and unclad buildings, as well as specific structural elements, force and pressure coefficients were included. Force coefficients (drag coefficients) were given for frames, lattice towers, walls and hoardings. An analysis approach was also added for analysing the dynamic response of flexible structures under wind loading using the gust response factor. This Code does not apply to structures such as chimneys, cooling towers, transmission line towers, or bridges. There are various Indian Standards for chimneys and cooling towers. The IRS and IRC Specifications provide information on bridges (just static forces). Specialist literature on bridge aerodynamics can be consulted. With substantial work being done worldwide in the area of wind engineering, there is growing body of new information. The user of this Code is advised to consult specialist literature for the design of large or important projects involving various types of structures

2.3 Reference Research paper and their Summaries

A. (Experimental and Numerical Study of Wind-Pressure Distribution on Irregular-Plan-Shaped Building) **by Biswarup Bhattacharyya and Sujit Kumar Dalui**

They presented a detailed analysis on an E-plan-shaped building that is asymmetrical around both plan axes when subjected to wind stimulation in this publication. The wind angle of incidence varied from 0° to 330° with a 30° gap. This research is carried out in a wind tunnel and numerically using the computational fluid dynamics (CFD) technique. The k- ω and shear stress transport (SST) k-models are used in the numerical analysis. They also conducted a rigorous investigation on a symmetrical E-plan shaped building with the same cross section area, looking for the greatest positive and negative

mean pressure coefficients as a result of a small aerodynamic alteration. The maximum positive mean Cp on some building faces was observed at skew wind angles, where the wind flow is not perpendicular to the building axis; however, the maximum negative mean Cp was observed at a far smaller number of skew wind angles. The asymmetry in the plan form about both axes causes this variation.

B. (Aerodynamic analysis of pentagon-shaped tall buildings) **by Najah Assainar and Sujit Kumar Dalui**

The efficiency of aerodynamic adjustments performed to a pentagonal-plan shaped model is investigated in this research study utilising computational fluid dynamics (CFD) simulation using the software package ANSYS CFX. Aerodynamic forms such as setback and tapering are studied as well as corner modifications such as chamfered, recessed, and rounded. efficiency.

According to the findings, the chamfered model is the most effective corner alteration in terms of pressure and force coefficients, as well as having outstanding dynamic performance. The study also found that among aerodynamic forms, the tapered model was better at decreasing pressure and force coefficients during static analysis. The dynamic analysis revealed a similar trend, with the exception of peak frequency, which was better predicted by the setback model.

C. (Wind tunnel study of wind effects on a high-rise building at a scale of 1:300) **by R. Sheng and L. Perret**

The objective of this work is to use wind-tunnel testing on a high-rise building with a well-defined atmospheric boundary layer at a 1:300 scale to investigate the unstable properties of global and local wind loads, as well as their connections with the atmospheric boundary layer. Wind data include mean velocity profile, turbulence intensity, and power spectrum of the fluctuation for global and local wind loads is investigated. The findings of this study reveal that, depending on the location, the upstream flow or the shear layers that form at the building's upstream corners, or both, influence wall-pressure pressures on the tower.

The loss of the strong spectral signature for the global wind force in the longitudinal direction is attributed to the loss of phase coherence between pressure signals on these sides, according to an investigation of spectral coherence between wall-pressure data at different pressure tap positions.

D. (Experimental study of wind-induced pressures on tall buildings of different shapes) **by Suresh K Nagar and Ritu Raj**

In this paper, mean wind pressure coefficients of a square and H-plan shaped tall buildings are investigated using wind tunnel testing. The experiment was conducted for various wind direction angles from 0^{o}, 30^{o}, 60^{o} and 90^{o} and for various identical building interference conditions. In order to investigate the interference effects, interfering factor were calculated. Different interference conditions taken under consideration were Full blockage, Half blockage, No blockage.

Non-dimensional interference factors (IF) represent the aerodynamic pressures on a plan-shaped major building with interference from nearby plan-shaped buildings and are used to illustrate interference effects. They proposed that the value of mean wind pressure coefficient decreases with an increase in the wind incidence angle up-to an angle of 60^{o}. Suction starts after further increase in wind incidence angle. The interference factor in both the models is less than unity. The interfering building at full blockage generates more suction compared to other two condition. The configuration of the interfering in no blockage condition caused almost no effect on mean pressure coefficient for square shaped building while it's reduced to almost 50% in case of H shape building.

E. (Comparison of aerodynamic coefficients of various types of Y-plan-shaped tall buildings) **by Prasenjit Sanyal1 · Sujit Kumar Dalui2**

The outline of a Y-plan structure is tri-axially symmetrical, with three independent wings connected to a central core part. The influence of major shape alterations (taper, helix, setback) and minor shape modifications (chamfered corner, recessed corner, rounded corner) on a Y-plan-shaped building was statistically evaluated using the computational fluid dynamics (CFD) technique in the current study. For different angles of attack, the wind force and pressure of different Y buildings have been calculated more precisely (AOAs). The setback building with a fully rounded corner outperforms the other variants in terms of minimising wind load and overturning moment coefficient. They discovered that the k–epsilon and SST turbulence models predict nearly identical maximum aerodynamic coefficients.

F. (Effects of Aerodynamic Modifications of Building Shapes on Wind Induced Response of Tall Buildings) **by Kwok and Bailey (1987)1, Kwok et al (1988)2**

Kwok and Bailey (1987), Kwok et al (1988), and Kwok (1988) conducted wind tunnel tests to evaluate the effects of aerodynamic devices, building edge configuration, and through building opening on wind induced vibrations in tall structures. Horizontal slots, slotted corners, and chamfered corners have all been found to be beneficial in reducing in both the dynamic along wind and crosswind responses of the rectangular cross-section CAARC Standard Tall Building.

G. (Effects of Side Ratio on Wind-Induced Pressure Distribution on Rectangular Buildings) **by J. A. Amin1 and A. K. Ahuja**

The findings of wind tunnel tests on 1:300 scaled-down models of rectangular buildings with the same plan area and height but varying side ratios ranging from 0.25 to 4 are described in this study. Wind pressures fluctuate, hence mean, maximum, minimum, and r.m.s. values of pressure coefficients are calculated at pressure locations on all surfaces of models. At a wind incidence angle of 0 to 90 at a 15-degree interval, the effectiveness of side ratios of models in changing the surface pressure distribution is evaluated. They came to the conclusion that the did ratio of models has a significant impact on the amount and distribution of wind pressure on leeward and sidewalls, but only a little impact on windward walls when the wind incidence angle is zero. Changes in side ratio have little effect on the general magnitude of peak pressures and peak suctions in building models with constant cross section, but they do influence the wind angle at which they occur.

H. (Wind pressure and velocity pattern around 'N' plan shape tall building) **by A. Mukherjee and A. K. Bairagi**

Mukherjee et al. (2017) studied the wind pressure and velocity pattern around 'N' shaped tall buildings. The paper is centred around determining the wind pressure coefficient and wind velocity analysis of the building using k-ε methods.

I. (Modelling of Wind Pressure Coefficients on C-Shaped Building Models) b**y M. Mallick, A. Mohanta, A. Kumar, and V. Raj**

Monalisa Mallick et al. (2018) studied the simulation of the wind pressure coefficient on C-shaped building models by means of numerical analysis using ANSYS Fluent and concluded that the pressure on the building was remarkably influenced by the structure geometry, orientation, aspect ratios, and wind angle of attack.

J. (On the domain size for the steady-state CFD modelling of a tall building) by **J. Revuz1, D.M. Hargreaves*2 and J.S. Owen2**

Revuz and D.M. Hargreaves (2012) investigated on the size of domain size for conducting CFD in the field of wind engineering. This paper discussed about what size of domain to use while using CFD tools for simulation of tall buildings.

K. (Recommendations on the use of CFD in wind engineering) by **Jörg Franke and Charles**

This study examines the results of published simulations and makes recommendations for the use of CFD in wind engineering jobs, with a focus on statistically steady wind simulation. To make recommendations on the proper use of CWE for that purpose, this work summarised the results for mean velocities and turbulence in the constructed environment from statistically steady RANS simulations accessible in the literature.

L. (Wind tunnel and full-scale study of wind effects on China's tallest building) by **(Q.S. Li, J.Y. Fu, & Y.Q. Xiao)**

They used wind tunnel testing and full-scale field observations to study the effects of severe winds on the Jin Mao Building in this paper. Wind response and wind-induced loads of this super tall building were shown and addressed in detail in the wind tunnel tests, including force coefficients, power spectrum densities, rms displacements, and rms accelerations. During the passage of Typhoon Rananim, however, full-scale

observations of wind effects on the Jin Mao Building were made. During the storm, field data such as wind speed, wind direction, and acceleration responses were continually captured.

M. (Streamlining meshing methodologies for annual urban CFD simulations, 2020) by **Patrick Kastner and Timur Dogan**

They estimated the time saving methodology that are possible along with specific mesh properties to take lead of the proposed method. They designed a circular mesh for urban wind simulations in this paper. They compared the box-shaped computational domain to the cylindrical simulation domain and found that if no annual wind analysis is required, the box-shaped approach is preferable. A cylindrical simulation domain is likely to outperform a box-shaped simulation domain.

N. (Experimental study of wind-induced pressures on tall buildings of different shapes, 2020) **by Ritu raj** investigated on H shape and square shape buildings under isolated as well as interference condition due to surrounding buildings. They examined mean pressure coefficient using wind tunnel experiment for various angle of attack of wind.

O. (Comparative study of wind induced mutual interference effects on square and fish-plan shape tall buildings, 2021**) by Pal Supriya, Ritu Raj discussed** wind-induced mutual interference effects on twin Square and Fish- plan shape building models having equal volume. They looked at the maximum efficiency for both shapes in terms of induced wind pressure and base shear and came up with the most efficient condition.

3 Methodology

DESIGN WIND PRESSURE

As per IS-875 Part 3,

[Design Velocity] = V_b*K_1*K_2*K_3*K_4

Where, V_b=Basic Wind velocity

K_1= Probability Factor/Risk Coefficient

K_2=Terrain and Height Factor

K_3=Topography Factor

K_4=Importance factor of the cyclonic region

Design wind pressure is given as:

$$\mathbf{P_d = 0.6\ [V_z]\text{^}2}$$

The mean pressure coefficient '$C_{p\ mean}$' is calculated from the equation given below:

$$\mathbf{C_{p\ mean} = \frac{(p - p_o)}{\frac{1}{2}\rho U_H{}^2}}$$

where p is the pressure at point on surface
p_o is the reference height static pressure,
ρ is the air density
U_H is mean wind velocity at the building reference height.

Modelling

In this study, ANSYS Designer Modular is used to model the similar wind tunnel condition to simulate the results. These simulated results are to be used for estimating the wind effect response on the building.

4 Numerical simulation using ANSYS

In this study, rectangular plan shaped buildings with different side ratios are analyzed by using ANSYS CFX package for CFD simulation. All the models analyzed are of same plan area 900m^2 and height 90m modeled on a scale of 1:100. The wind profile boundary layer is governed by power law equation. efficient.

Table 4-1 Prototype and Model Dimension

Modal shape	Prototype Dimension(m)	ANSYS Model Dimension(mm)	Height of Model (mm)	Scale of Model
Square	30*30	300*300	900	1:100
Rectangle-1	36*25	360*250		
Rectangle-2	45*20	450*200		
Rectangle-3	60*15	600*150		

The models are rotated from 0° to 90° at 30° interval. Therefore, attacking wind angles are 0°, 30°, 60°, 90°. This study also validates with wind pressure of an isolated square plan shape, tall building using CFD simulation and compared it with wind effects of conventional plan shape building given in Indian code IS: 875 (Part- 3), 2015.

MEAN WIND PROFILE with HEIGHT

Due to the roughness of earth surface, there acts a drag force on wind flow near the ground. This effect gradually decreases as the height increases and at a certain gradient level (around 400m), this drag-force becomes negligible. The degree of surface roughness and drag caused by surrounding projections that oppose wind flow determine the vertical profile of wind speed. Gradient height is the height at which the drag effects disappear, while gradient velocity is the corresponding velocity. The height up-to which wind speed is influenced by topography is called atmospheric boundary layer.

POWER LAW

As per Power Law, the wind speed profile within the atmospheric boundary layer is given by:

$$\frac{V}{Vo} = \left[\left(\frac{Z}{Zo}\right) \text{^} \left(\frac{1}{alpha}\right)\right]$$

Where, V = velocity of wind at height Z

Vo = gradient velocity of wind at reference height Zo

Z = height above ground

Zo = Nominal height of Boundary layer (also called gradient height)

alpha = power law coefficient.

LOGARITHMIC LAW

$$u = \frac{1}{k} u_* \ln \frac{Z}{Z_0}$$

where u is the wind speed at height Z above ground,

k is the von Karman constant equal to 0.4 (approximately)

and Zo is the ground roughness.

u_* is shear velocity which is defined as:

$$u_* = \sqrt{\frac{\tau_0}{\rho}}$$

where τ_0 is the stress of wind at ground level and ρ is the air density.

4.1 CFD Validation

The validity of the ANSYS CFX software is validated before beginning the numerical study of the building. For this purpose, a square plan shaped building with dimensions of 100 mm ×100 mm and a height of 500 mm (i.e., aspect ratio 1:5) is investigated using the k-model with ANSYS CFX in the domain under uniform wind flow.

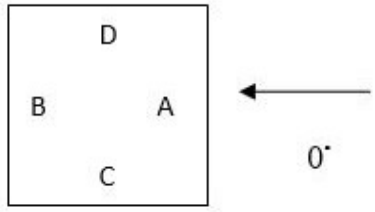

Figure 4-1 Different faces of the model with direction of wind

At the inlet, a uniform wind flow of 10 m/s is given. As previously stated, the domain is built according to Revuz et al (2010). The ANSYS CFX programme determines the face average values of coefficient of pressure, which are then compared to wind action codes from various regions.

Table 4-2 Comparison of face average values of coefficients of pressure

Wind loading code	**Face- A**	**Face-B**	**Face-C**	**Face-D**
By ANSYS CFX	0.75	-0.49	-0.69	-0.68
ASCE 7-10	0.8	-0.5	-0.7	-0.7
AS/NZS-1170.2(2002)	0.8	-0.5	-0.65	-0.65
IS: 875 (part3) (2015)	0.8	-0.25	-0.8	-0.8

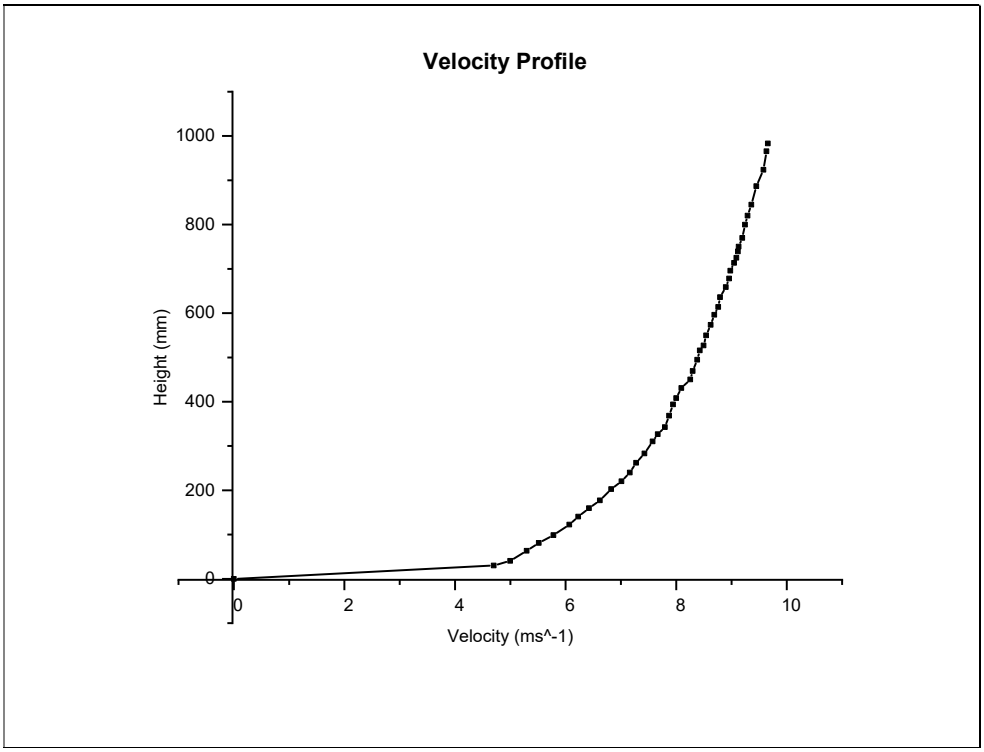

Figure 4-2 Velocity profile

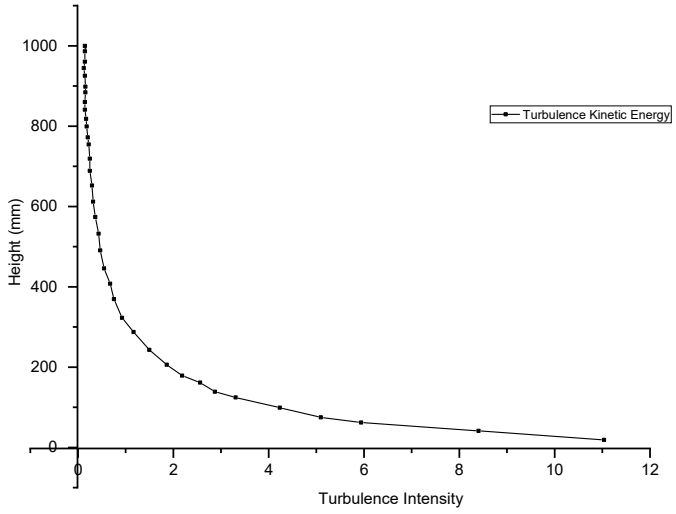

Figure 4-3 Turbulence Intensity

Domain

In case of high-rise buildings, domain size is mainly governed by height of the building such that a large number of cell count could be formed and out of them, many being used up in the region far away from wake region.

Domain size selected in modeling is defined as per frank et al (2004), The inlet and outlet distance of the domain from the building position is taken as 5H and 15H, respectively. The side aspect and top clearance are also taken as 5H, where H is the height of the building. The domain configurations are depicted in Fig.

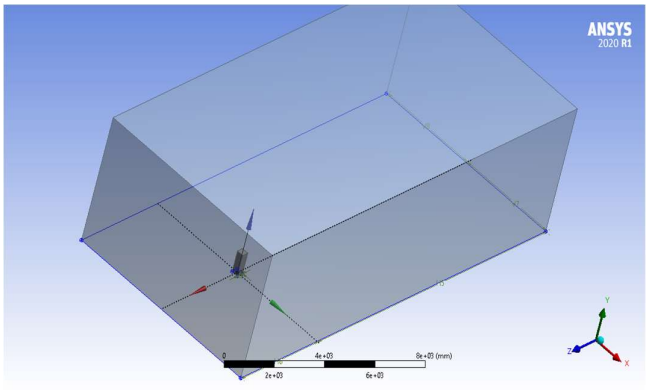

Figure 4- 4-4 Domain (virtual wind tunnel)

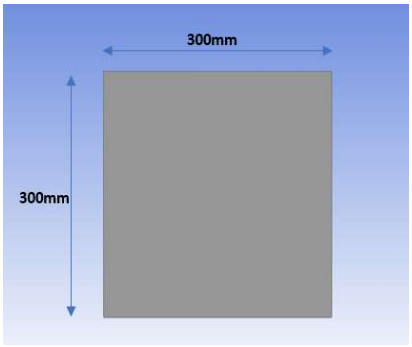

Figure 4-5 Model 1 Dimension

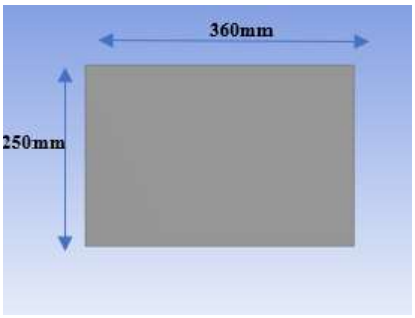

Figure 4-6 Model 2 Dimension

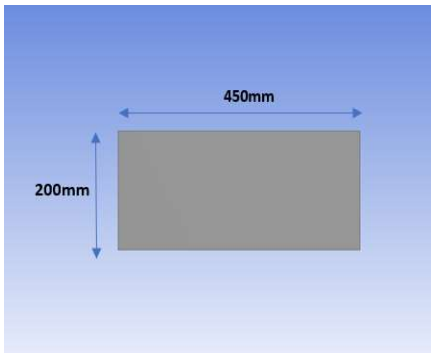

Figure 4-7 Model 3 Dimension

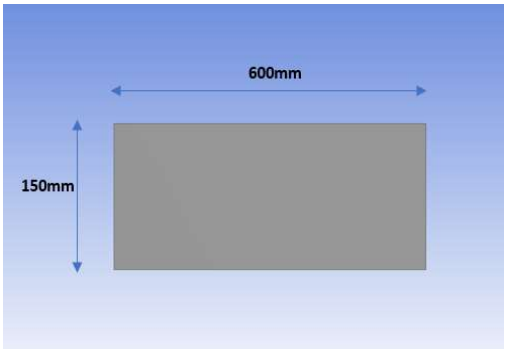

Figure 4-8 Model 4 Dimension

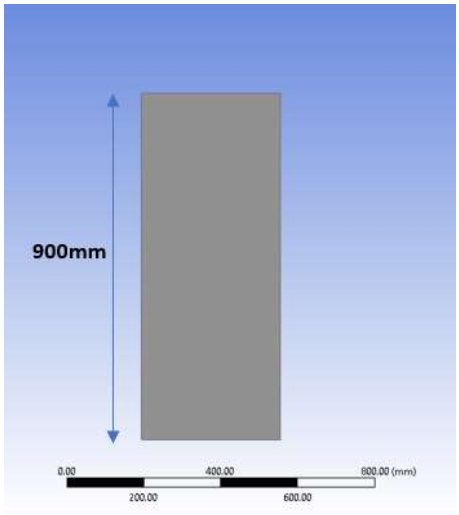

Figure 4-9 Height of Model

MESHING

Meshing is an integral part of engineering simulation process where complex geometries are divided to simple elements that can be used as discrete local approximations of larger domain.

Meshing influences the accuracy, convergence and speed of the simulation. Finer the mesh, better the accuracy.

Types of Mesh

A. Tetrahedron Meshing
B. Pyramid Meshing
C. Hexahedron Meshing
D. Polyhedron Meshing
E. Prism Meshing

The meshing in domain is done by tetrahedral mesh elements. Meshing near the buildings are made comparatively finer for enhancing the accuracy of results. The velocity at the inlet is taken as 10 m/s. No slip condition is defined for side walls and ground.

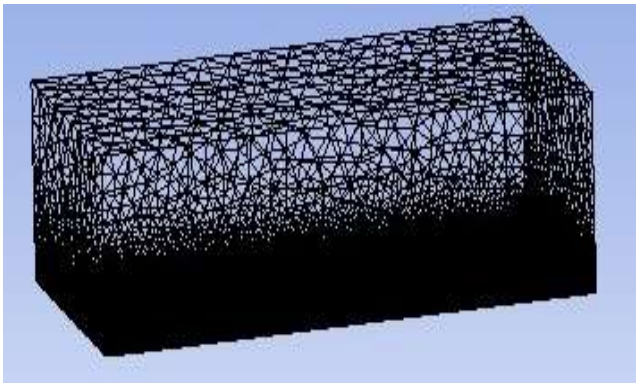

Figure 4-10 Domain Meshing

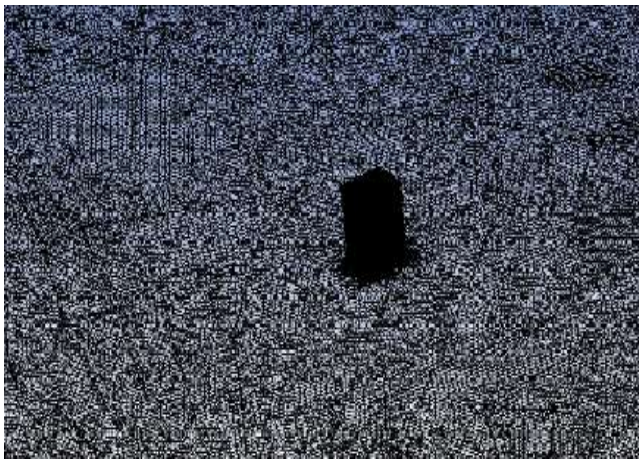

Figure 4-11 Building Meshing

4.2 **Governing Equations**

K-ε turbulence model is used to simulate mean flow characteristics for model. This model uses two equation model by means of two transport equations. The k-ε model uses the gradient diffusion hypothesis to relate the Reynold stresses to the mean velocity gradients and turbulent viscosity. Here, k is turbulence kinetic energy and is defined as the variance of fluctuations in velocity and Ɛ is the turbulence eddy dissipation (the rate at which the velocity fluctuation dissipates).

For a turbulence model used, instantaneous velocity can be written as the summation of time averaged mean velocity and a time varying fluctuating component given as below:

$$u_i = U_i + u_i'$$

where, u_i = instantaneous velocity

U_i = time averaged mean velocity

u_i' = fluctuating component of velocity

As per Reynold's Average Navier Stokes Equation (RANS) equation:

$$\frac{\partial}{\partial x_i}(\rho U_i) = 0$$

where, ρ = density of fluid

and conservation of momentum equation can be written as,

$$\frac{\partial}{\partial x_j}(\rho U_i U_j) = -\frac{\partial P}{\partial x_i} + \frac{\partial}{\partial x_f}\left[\mu\left(\frac{\partial U_i}{\partial x_j} + \frac{\partial U_f}{\partial x_i}\right)\right] + \frac{\partial}{\partial x_j}\left(-\rho\overline{u_i' u_j'}\right)$$

5 RESULTS AND DISCUSSION

The external pressure coefficient is calculated by using the expression,

$$C_{pe} = \frac{P}{0.6 \times V_z^2}$$

5.1 Pressure Distribution

Pressure distribution for various faces of building is shown using contour plots as below:

1. **Model- 1 Square shaped Building**

- The pressure contours for different faces at various angle of incidence depicts the pressure distribution on faces and are shown in figures.
- Initially, at 0 degree of incidence face A shows a positive pressure being the windward face whereas face B, C, and D depicts a negative pressure distribution being the leeward and side wall face of the building.
- As the angle of incidence changes to the pressure distribution changes and so the pressure coefficient.
- For 30° and 60° angle of incidence, positive pressure distribution at face A become slightly less compared to what in case of 0° along with suction pressure increase at face D and a comparable change can be viewed from the pressure coefficient data so obtained as a result.
- For 90° angle of incidence, face C become windward and similar contour plot pattern as of face A when angle of attack was 0° can be seen.

1. Zero-degree Contour Plots

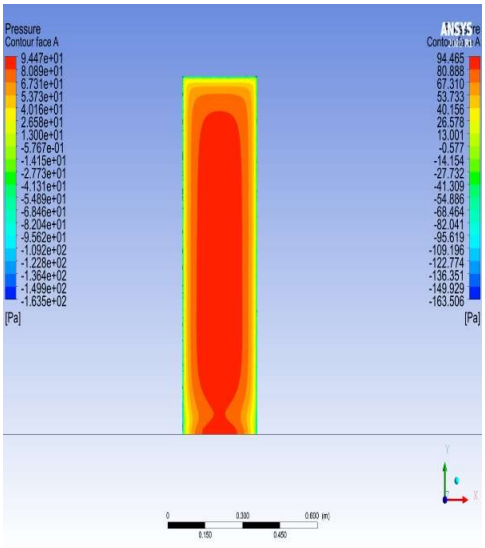

Face A

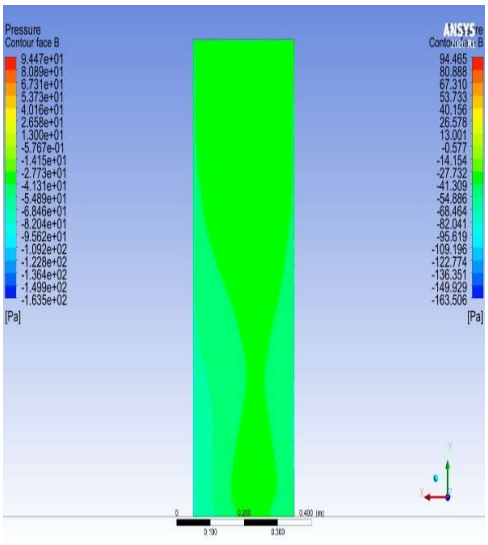

Face B

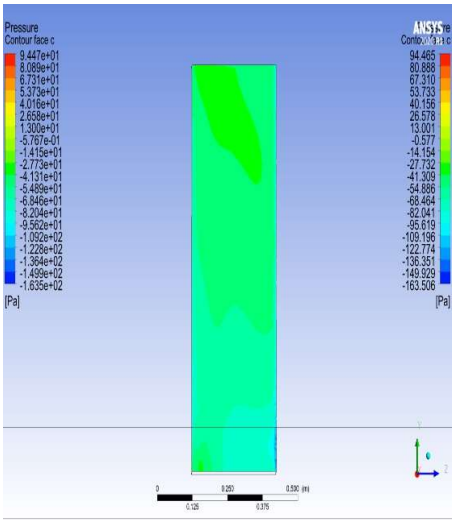

Face C

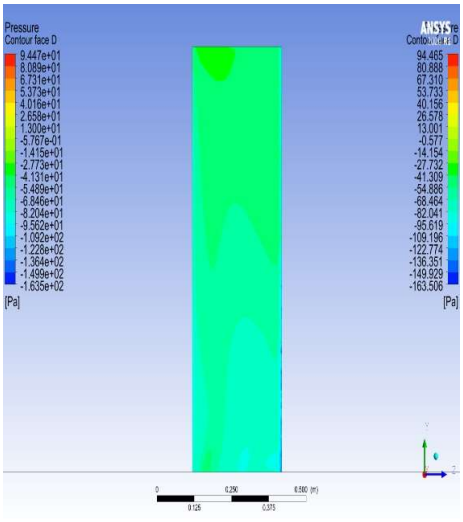

Face D

Figure 5-1 Contour Plots for different faces at 0- degree of incidence for Model 1

2. 30-degree Contour Plots

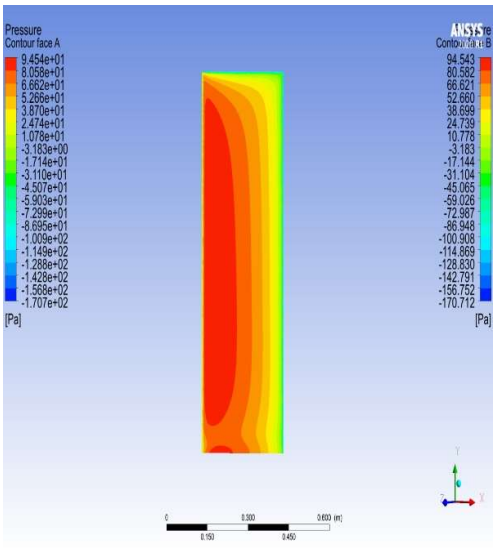

Face A

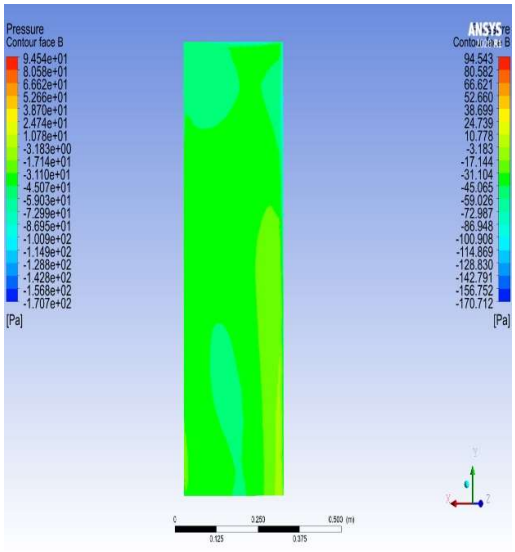

Face B

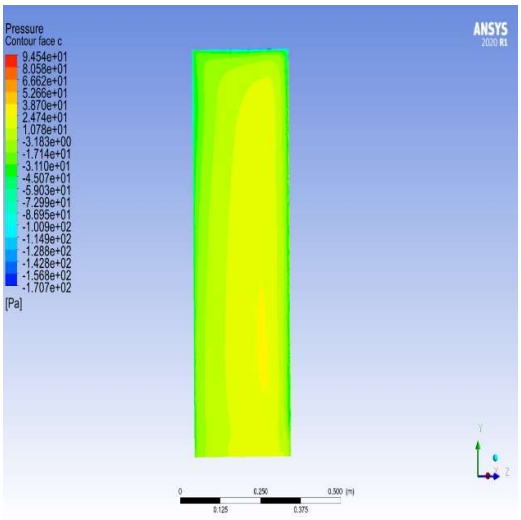

Face C

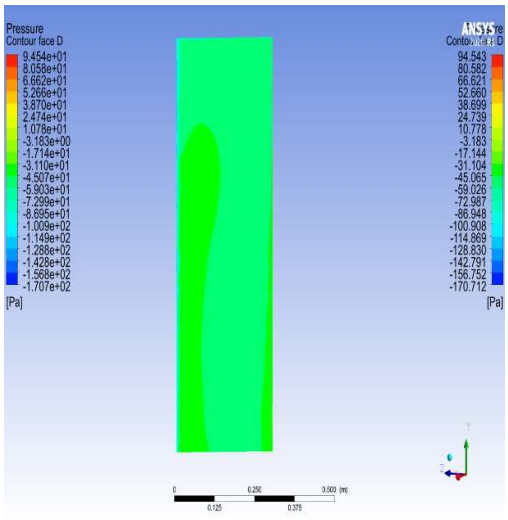

Face D

Figure 5-2 Contour Plots for different faces at 30- degree of incidence for Model 1

3. 60-degree Contour Plots

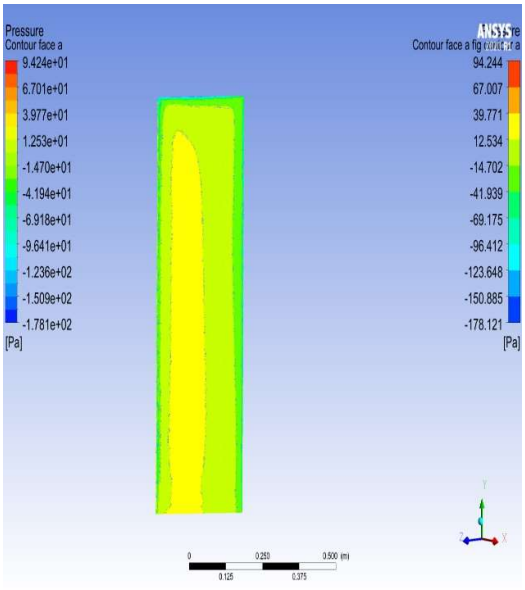

Face A

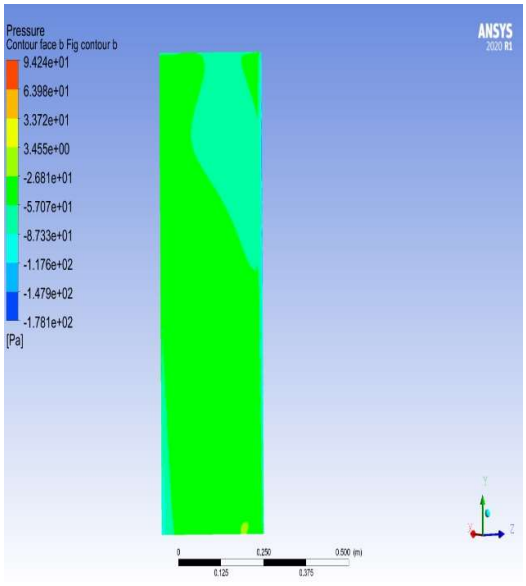

Face B

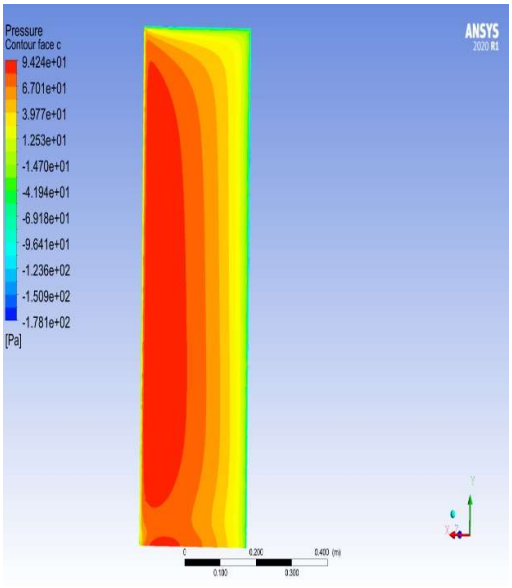

Face C

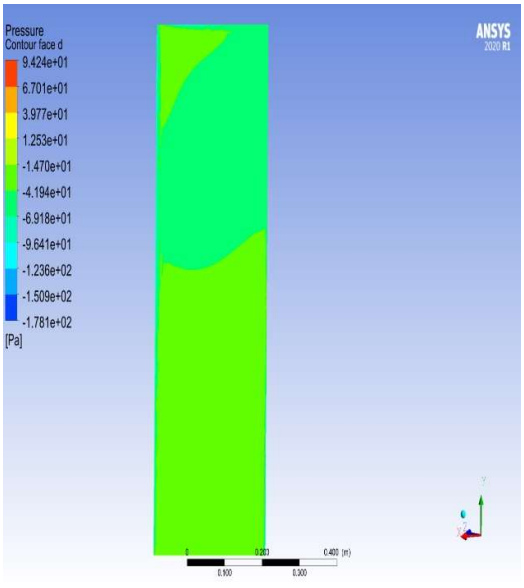

Face D

Figure 5-3 Contour Plots for different faces at 60- degree of incidence for Model 1

4. 90-degree Contour Plots

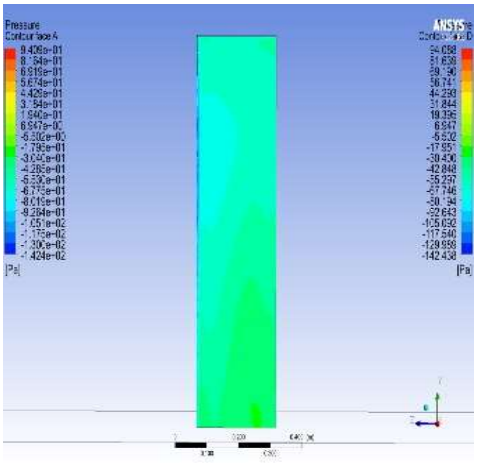

Face A

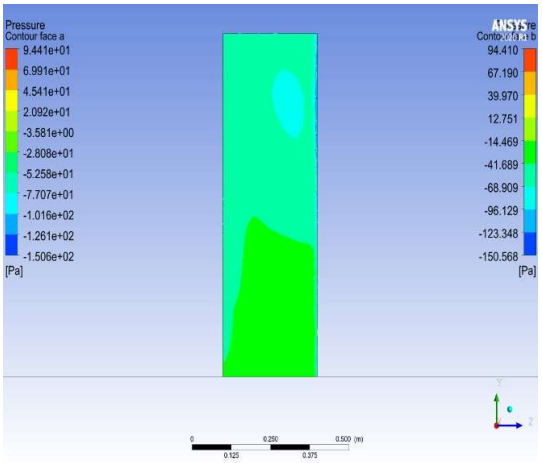

Face B

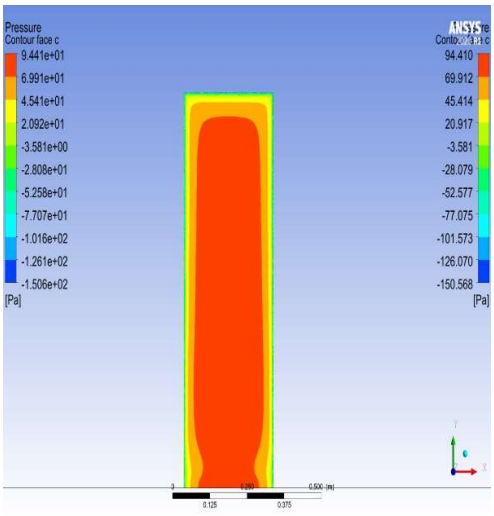

Face C

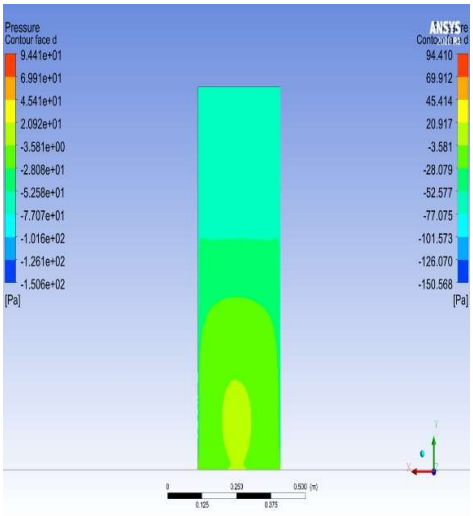

Face D

Figure 5-4 Contour Plots for different faces at 90- degree of incidence for Model 1

2. Model 2 Rectangular shape building with side ratio of 1.44

- Figures 5-5 to 5-8 exhibit the pressure distribution on different faces at varying angles of incidence.
- At 0 degrees of incidence, face A portrays a positive pressure distribution as the building's windward face, whereas faces B, C, and D depict a negative pressure distribution as the building's leeward and side wall faces.
- As the angle of incidence changes, the pressure distribution changes and so the pressure coefficient.
- For 30° and 60° angle of incidence, positive pressure distribution at face A become slightly less compared to what in case of 0° along with suction pressure increase at face D and a comparable change can be viewed from the pressure coefficient data so obtained as a result.
- For 90° angle of incidence, face C become windward and similar contour plot pattern as of face A when angle of attack was 0° can be seen.

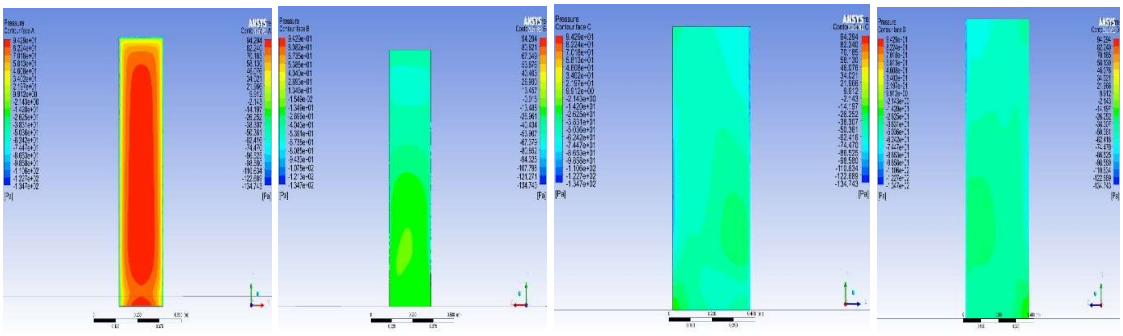

Face A **Face B** **Face C** **Face D**

Figure 5-5 Contour Plots for different faces at 0- degree of incidence for Model 2

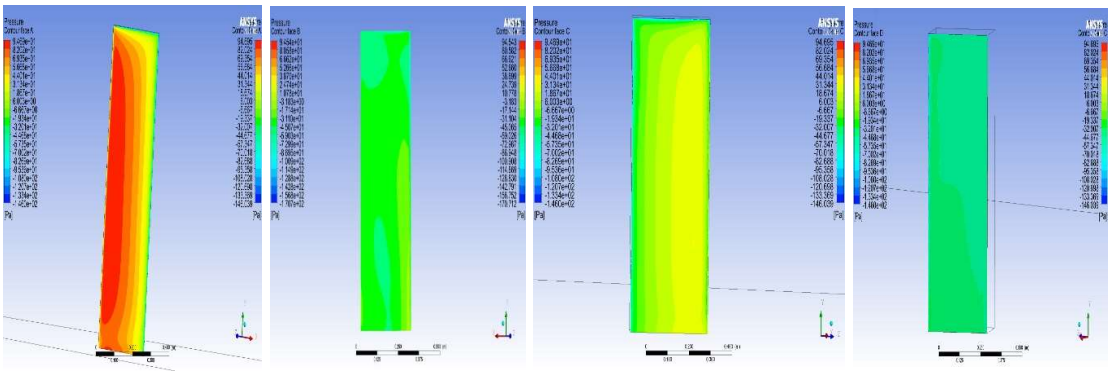

Face A **Face B** **Face C** **Face D**

Figure 5-6 Contour Plots for different faces at 30- degree of incidence for Model 2

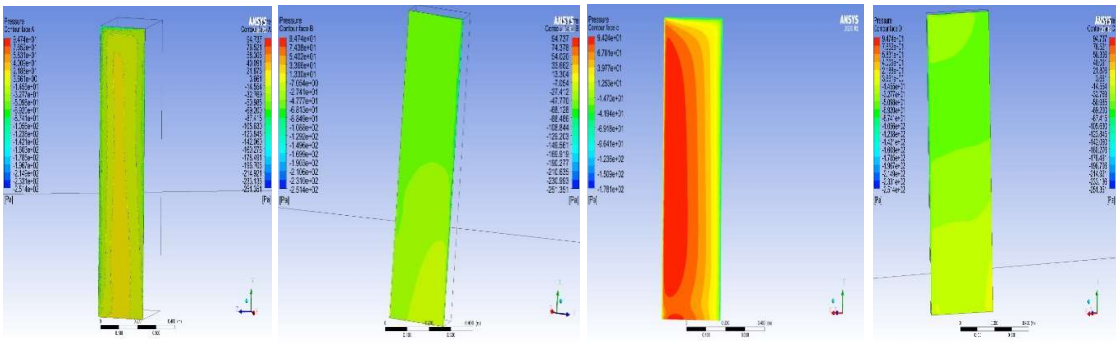

Face A **Face B** **Face C** **Face D**

Figure 5-7 Contour Plots for different faces at 60- degree of incidence for Model 2

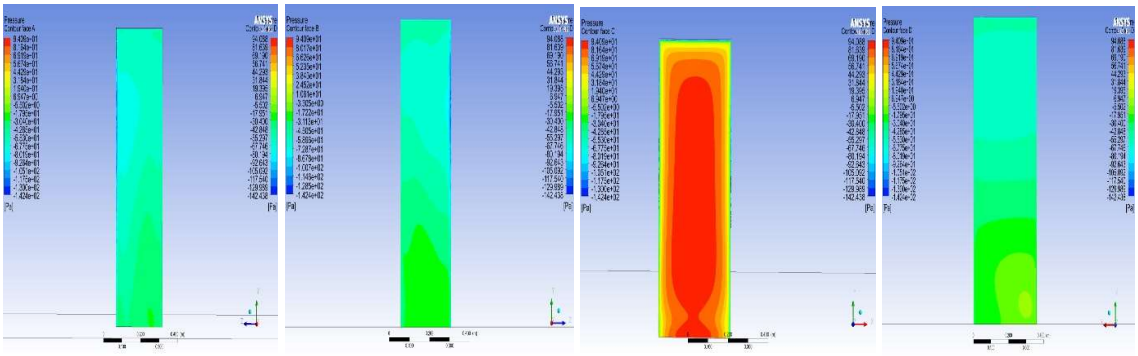

Face A **Face B** **Face C** **Face D**

Figure 5-8 Contour Plots for different faces at 90- degree of incidence for Model 2

3. Model 3 Rectangular shape building with side ratio of 2.25

- The pressure contours for different faces at various angles of incidence are depicted in fig. 5-9 to 5-12 and illustrated the pressure distribution on faces.
- At 30° and 60° angles of incidence, positive pressure distribution at face A is slightly less than at 0°, while suction pressure increases at face D, resulting in an equivalent change in the pressure coefficient data obtained as a result.
- When the angle of incidence is 90°, face C becomes windward and the contour plot pattern is similar to that of face A when angle of attack was 0°.

.

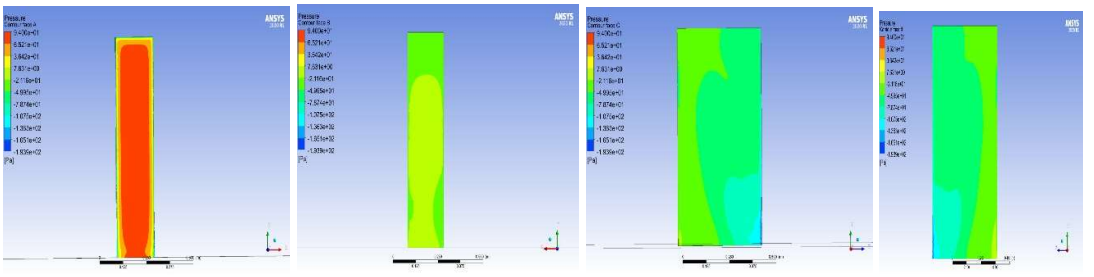

Face A **Face B** **Face C** **Face D**

Figure 5-9 Contour Plots for different faces at 0- degree of incidence for Model 3

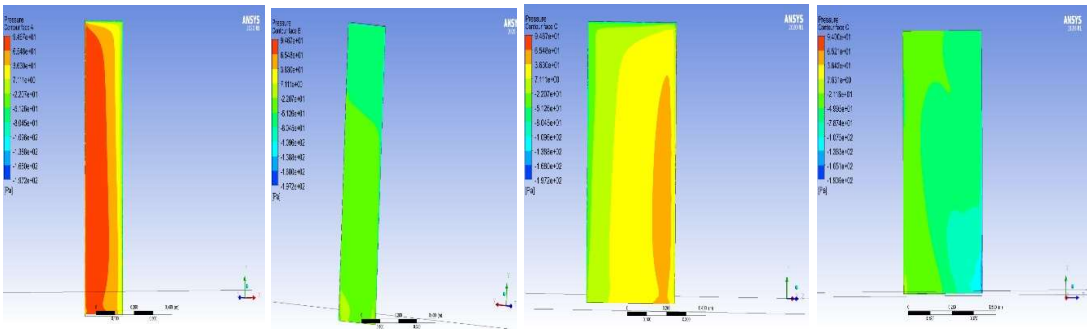

Face A **Face B** **Face C** **Face D**

Figure 5-10 Contour Plots for different faces at 30- degree of incidence for Model 3

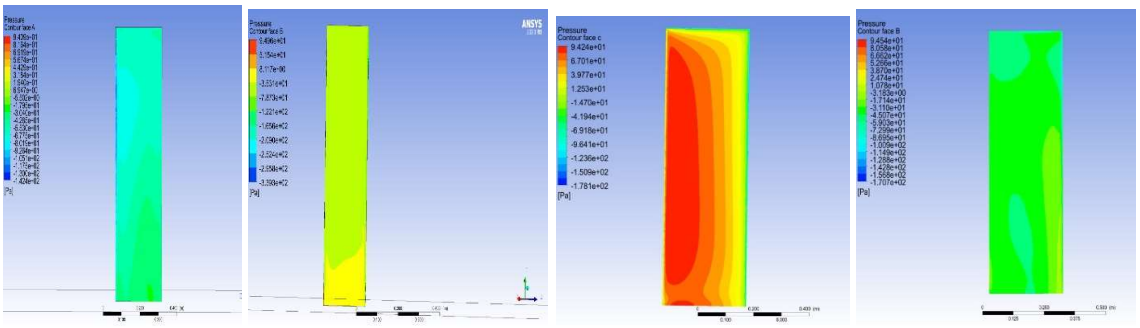

Face A **Face B** **Face C** **Face D**

Figure 5-11 Contour Plots for different faces at 60- degree of incidence for Model 3

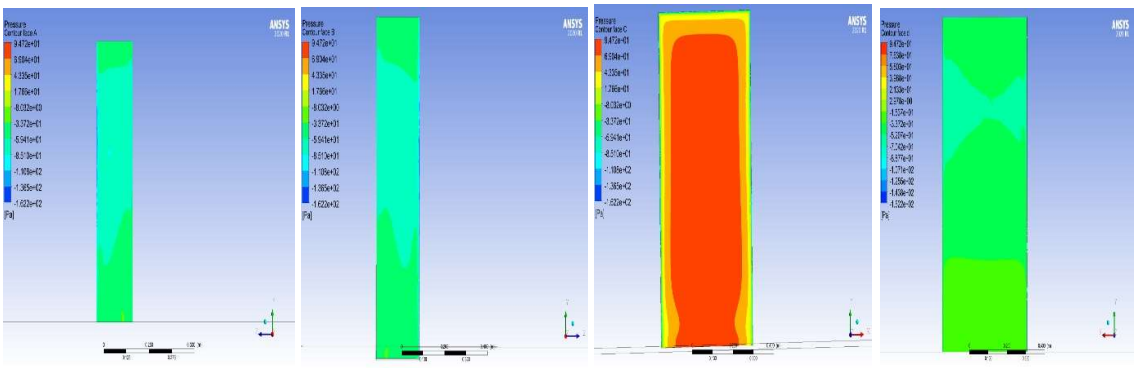

Face A **Face B** **Face C** **Face D**

Figure 5-12 Contour Plots for different faces at 90- degree of incidence for Model 3

4. Rectangular model with side ratio 4

Figures 5-13 to 5-16 exhibit the pressure distribution on different faces at varying angles of incidence. At 30° and 60° angles of incidence, positive pressure distribution at face A decreases slightly compared to 0°, while suction pressure rises at face D, and a comparable change can be seen in the pressure coefficient data.

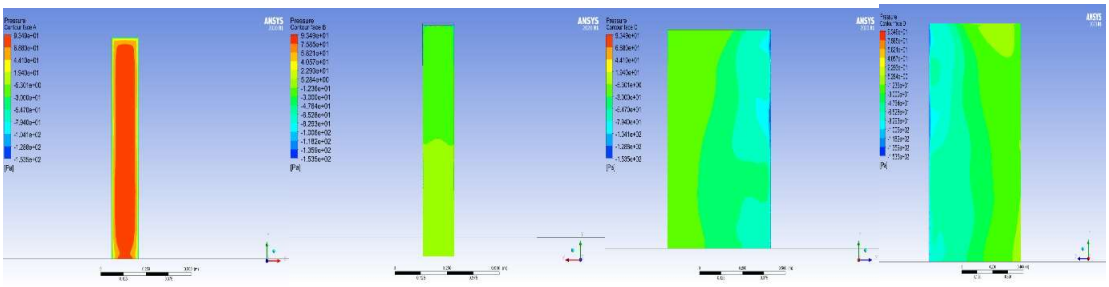

Face A **Face B** **Face C** **Face D**

Figure 5-13 Contour Plots for different faces at 0- degree of incidence for Model 4

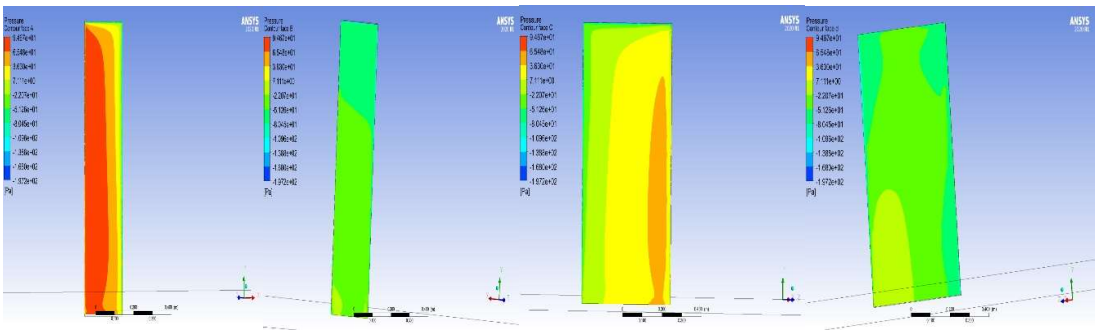

Face A **Face B** **Face C** **Face D**

Figure 5-14 Contour Plots for different faces at 30- degree of incidence for Model 4

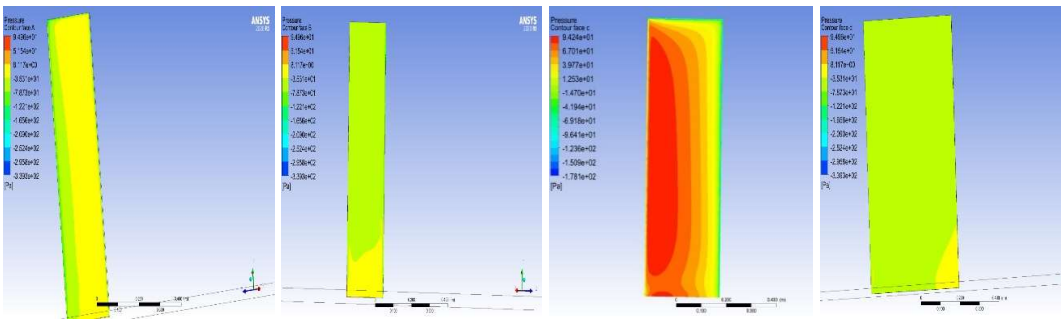

Face A **Face B** **Face C** **Face D**

Figure 5-15 Contour Plots for different faces at 60- degree of incidence for Model 4

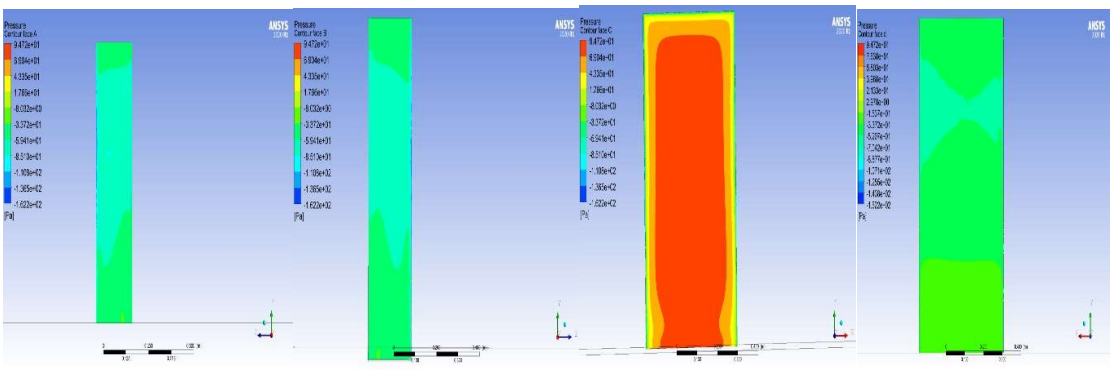

Face A **Face B** **Face C** **Face D**

Figure 5-16 Contour Plots for different faces at 90- degree of incidence for Model 4

5.2 Vertical Centerline Pressure Coefficients

The curve in these figures depicts the variation in the pressure coefficient Cp value for various faces as a function of height.

MODEL 1

- The curve in these figures 5-17 to 5-20 depicts the variation in the pressure coefficient Cp value for various faces as a function of height. Therefore, the face average value of Cp for several models at various angles of incidence are evaluated.
- For different faces A, B, C, D, the mean face average values of Cp at 0 ° angle of attack are +.75, -.49, -.69, and -.69, respectively.
- The face average Cp values for face A, B, C, and D at 30° are +.69, -.53, -.12, and -.66, respectively.
- The face average Cp values for face A, B, C, and D at 60° are -.31, -.58, +.51, and -.55, respectively.
- The face average Cp values for faces A, B, C, and D at 90° are -.68, -.65, +.68, and -.45, respectively.

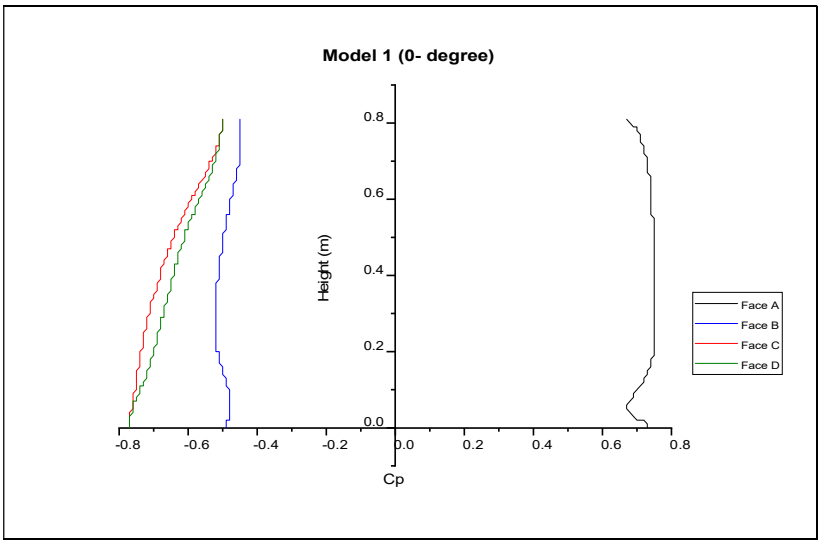

Figure 5-17 Pressure Variation along Centerline for all faces for 0-degree AOA of model 1

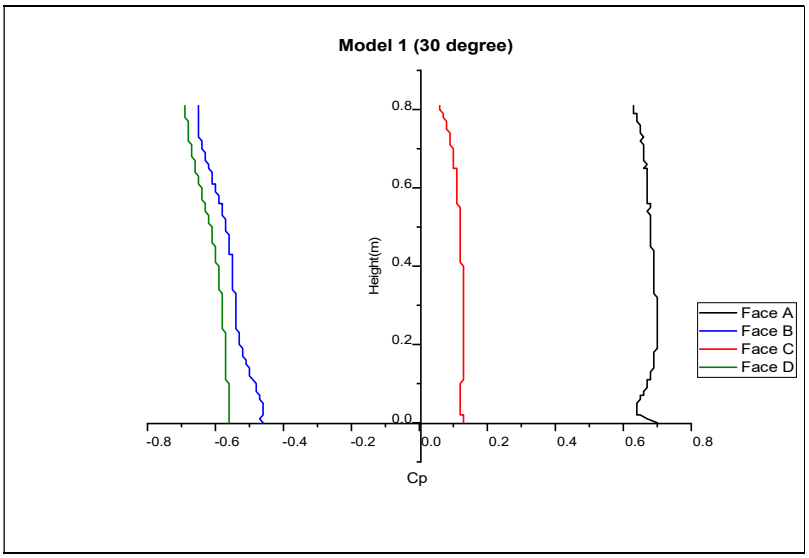

Figure 5-18 Pressure Variation along Centerline for all faces for 30-degree AOA of model 1

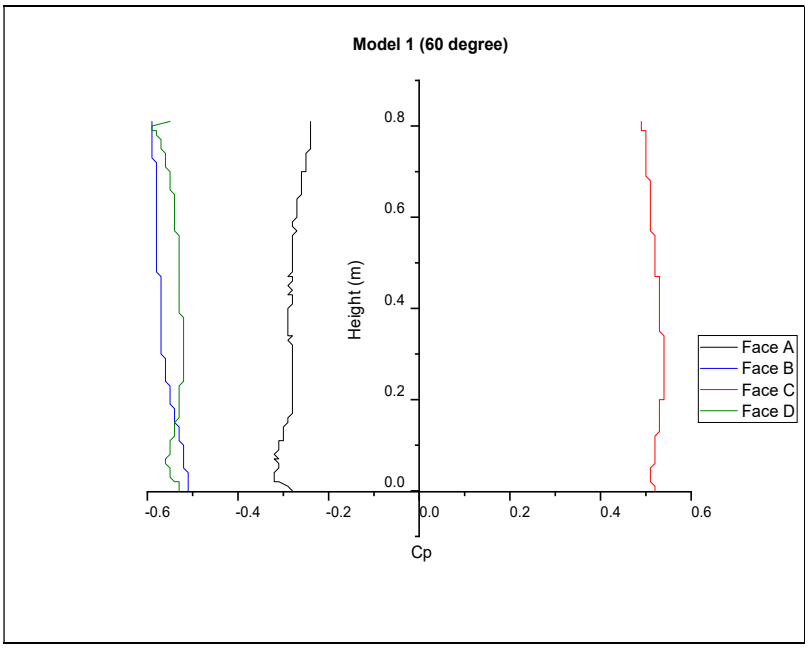

Figure 5-19 Pressure Variation along Centerline for all faces for 60-degree AOA of model 1

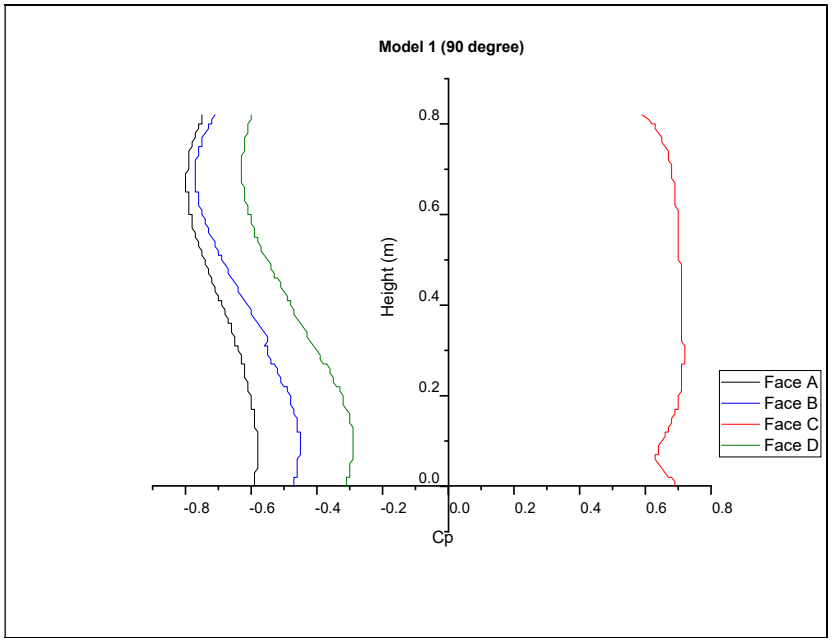

Figure 5-20 Pressure Variation along Centerline for all faces for 0-degree AOA of model 1

MODEL 2

In model 2, the face average value of Cp is calculated for various faces at various incidence angles. The Cp Variation along the centerline for all the faces at different angle of incidences are depicted in fig 5-21 to 5-24.

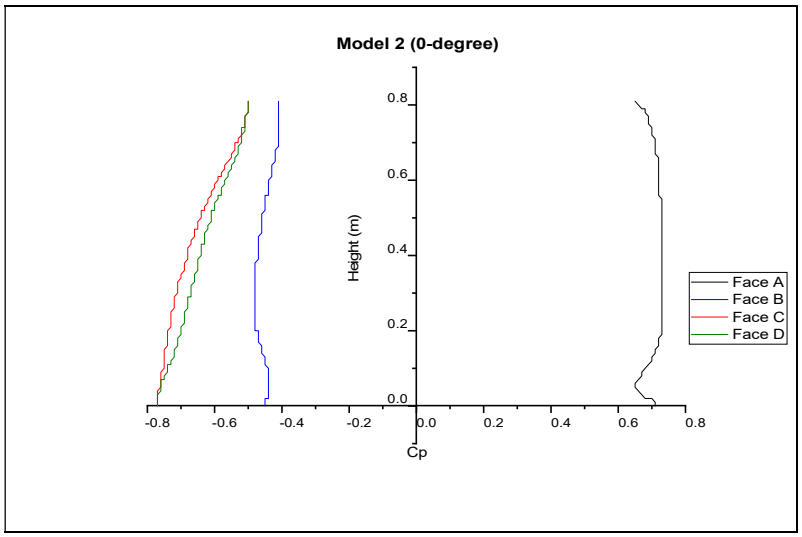

Figure 5-21 Pressure Variation along Centerline for all faces for 0-degree AOA of model 2

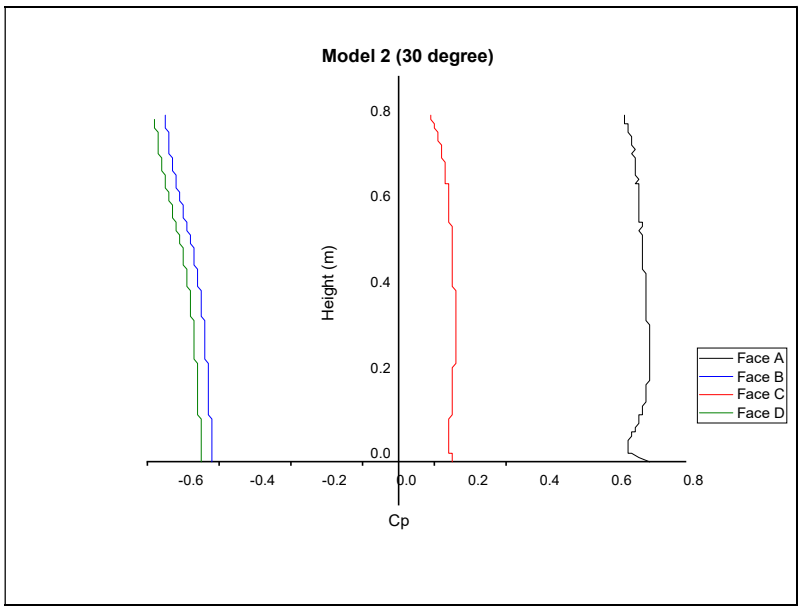

Figure 5-22 Pressure Variation along Centerline for all faces for 30-degree AOA of model 2

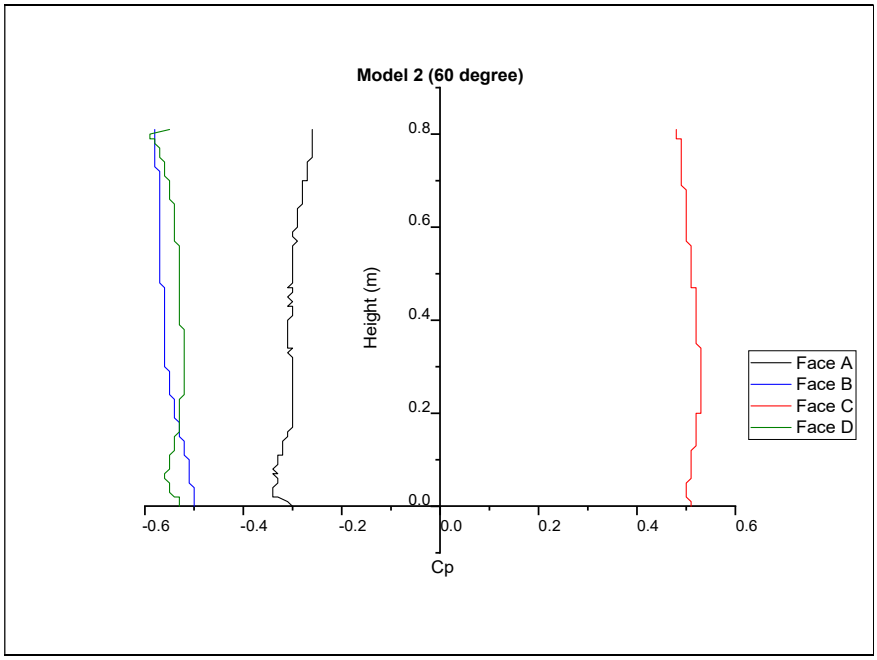

Figure 5-23 Pressure Variation along Centerline for all faces for 60-degree AOA of model 2

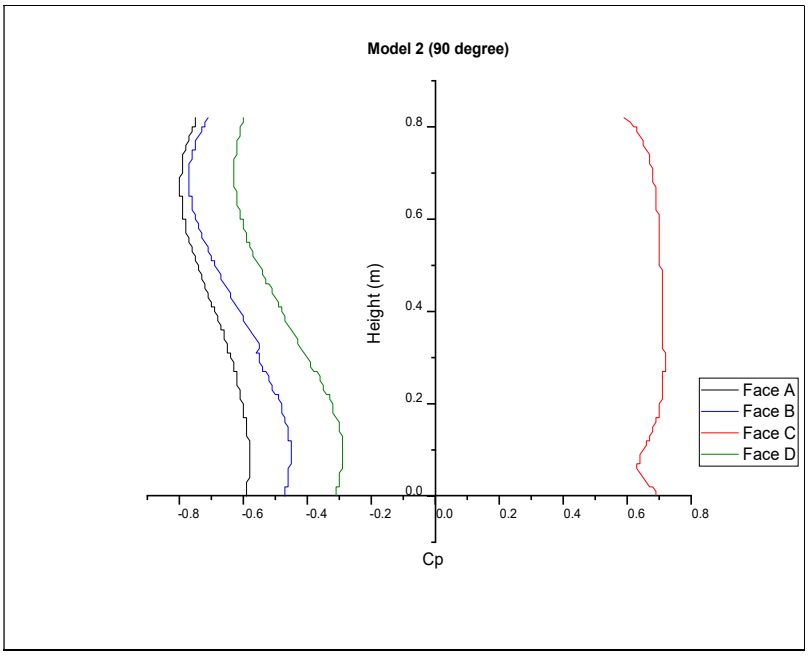

Figure 5-24 Pressure Variation along Centerline for all faces for 90-degree AOA of model 2

Model 3

- The Cp Variation along the centerline for all the faces at different angle of incidences are depicted in fig 5-25 to 5-28.
- For different faces A, B, C, D, the face average Cp at 0° AOA is +.74, -.35, -.62, -.62, respectively.
- The face average Cp values for face A, B, C, and D at 30° are +.68, -.47, -.15, and +.55, respectively.
- The face average Cp values for face A, B, C, and D at 60° are -.30, -.53, +.42, and -.49, respectively.
- Face average Cp values for face A, B, C, D for 90° are -.65, -.61, +.71, -.36 respectively.

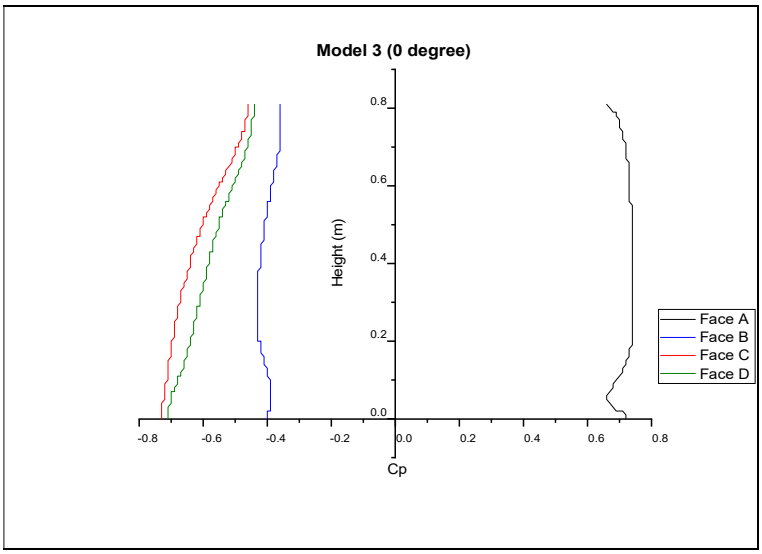

Figure 5-25 Pressure Variation along Centerline for all faces for 0-degree AOA of model 3

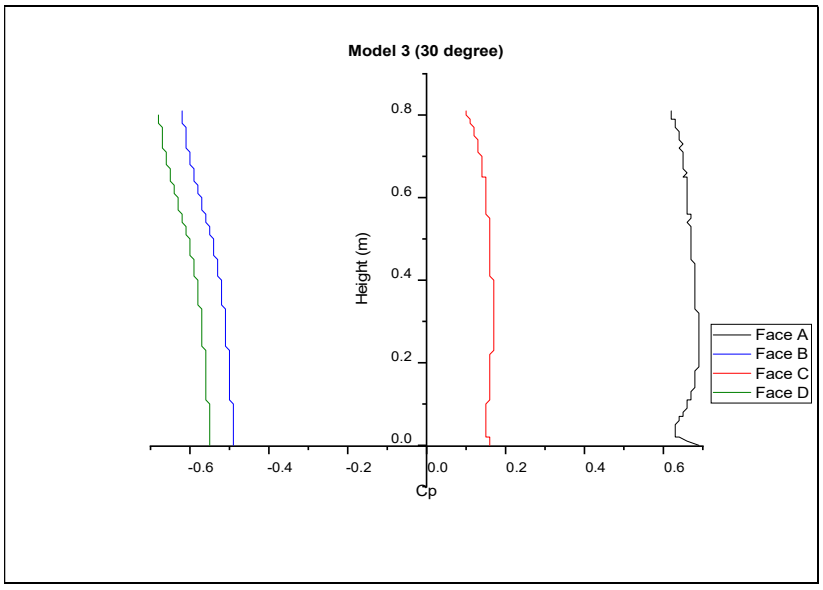

Figure 5-26 Pressure Variation along Centerline for all faces for 30-degree AOA of model 3

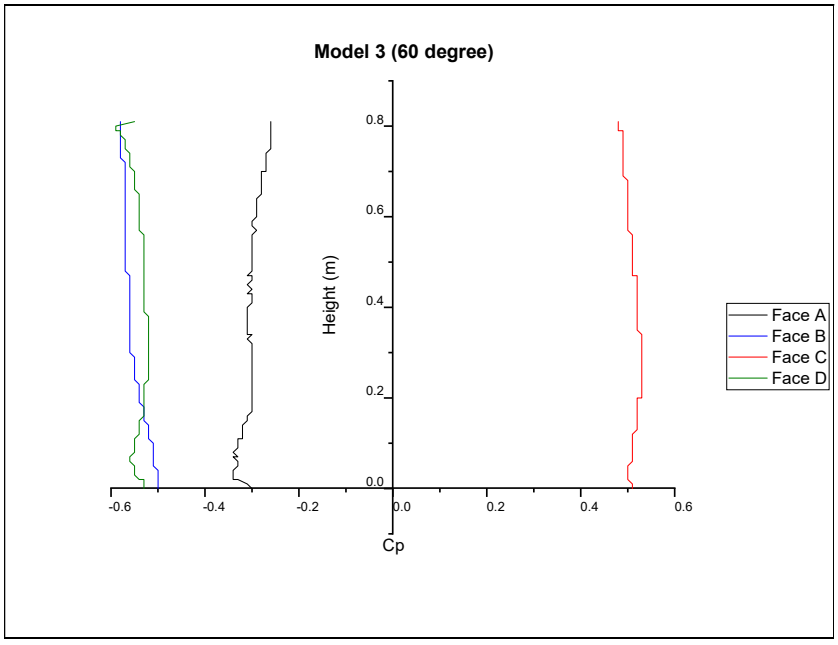

Figure 5-27 Pressure Variation along Centerline for all faces for 60-degree AOA of model 3

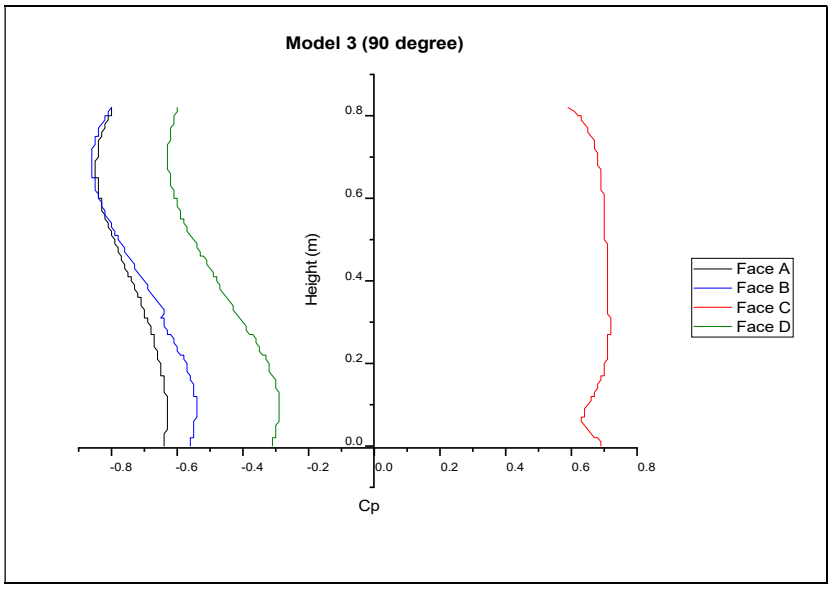

Figure 5-28 Pressure Variation along Centerline for all faces for 90-degree AOA of model 3

Model 4

- The Cp Variation along the centerline for all the faces at different angle of incidences are depicted in fig 5-29 to 5-32.
- For different faces A, B, C, D, the face mean Cp at 0 ° angle of attack is +.73, -.24,-.59, and -.59, respectively.
- The face average Cp values for face A, B, C, and D at 30° are +.67, -.44, +.17, and -.52, respectively.
- The face average Cp values for face A, B, C, and D at 60° are -.29, -.51, +.57, and -.41, respectively.
- The face average Cp values for face A, B, C, D at 90 degrees is -.61, -.58, +.74, -.21

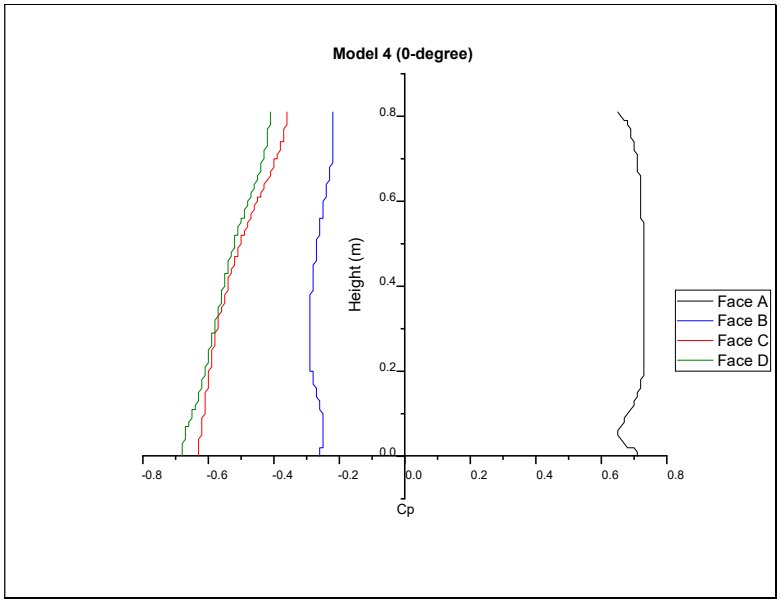

Figure 5-29 Pressure Variation along Centerline for all faces for 0-degree AOA of model 4

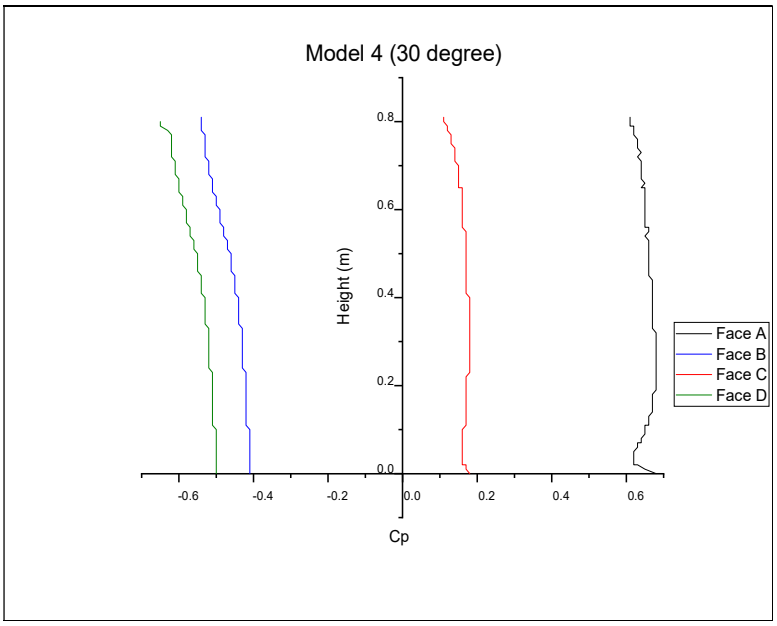

Figure 5-30 Pressure Variation along Centerline for all faces for 30-degree AOA of model 4

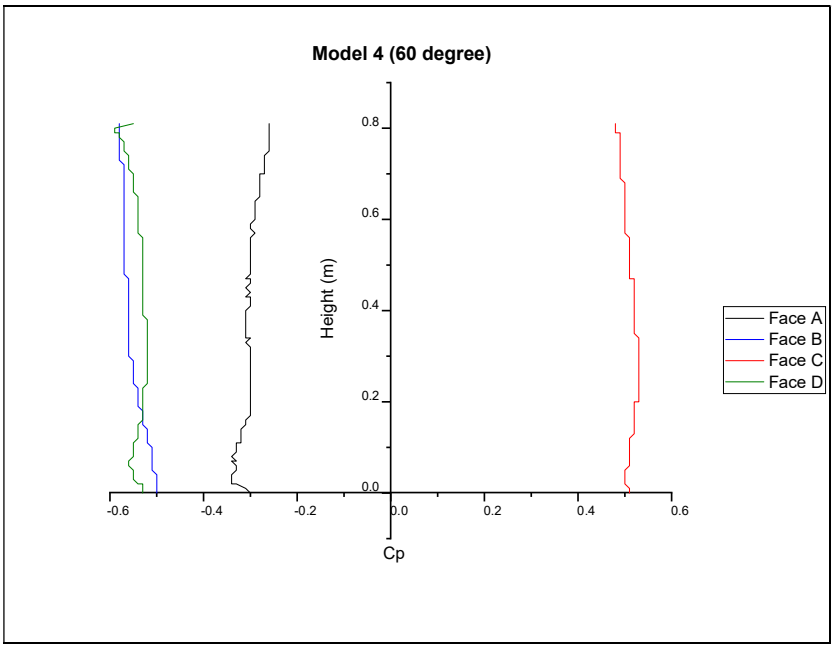

Figure 5-31 Pressure Variation along Centerline for all faces for 60-degree AOA of model 4

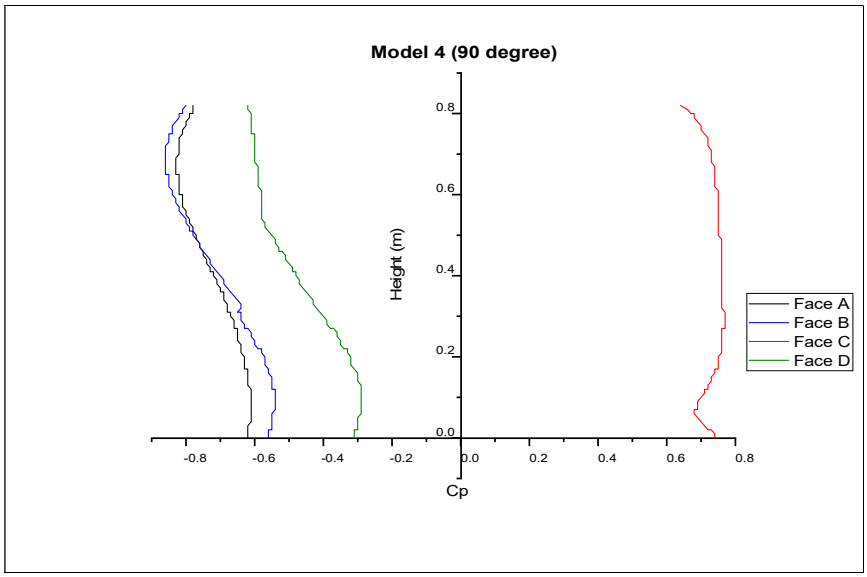

Figure 5-32 Pressure Variation along Centerline for all faces for 90-degree AOA of model 4

5.3 Pressure Coefficients

Table 5-1 Cp at 0-degree angle of incidence

Building model	Cp	Face A	Face B	Face C	Face D
Square	Mean	+0.75	-0.49	-0.69	-0.69
	IS-875	+0.8	-0.25	-0.8	-0.8
	AS/NZS	+0.8	-0.5	-0.65	-0.65
Rectangle-1	Mean	+0.74	-0.44	-0.66	-0.66
	IS-875	+0.8	-0.1	-0.5	-0.5
	AS/NZS	+0.8	-0.29	-0.65	-0.65
Rectangle-2	Mean	+0.74	-0.35	-0.62	-0.63
	IS-875	+0.8	-0.1	-0.5	-0.5
	AS/NZS	+0.8	-0.29	-0.65	-0.65
Rectangle-3	Mean	+0.73	-0.24	-0.59	-0.60
	IS-875	+0.8	-0.1	-0.5	-0.5
	AS/NZS	+0.8	-0.29	-0.65	-0.65

The mean pressure coefficient for different faces is evaluated and compared with the international standards for 0- degree angle of incidence as shown in fig 5-33.

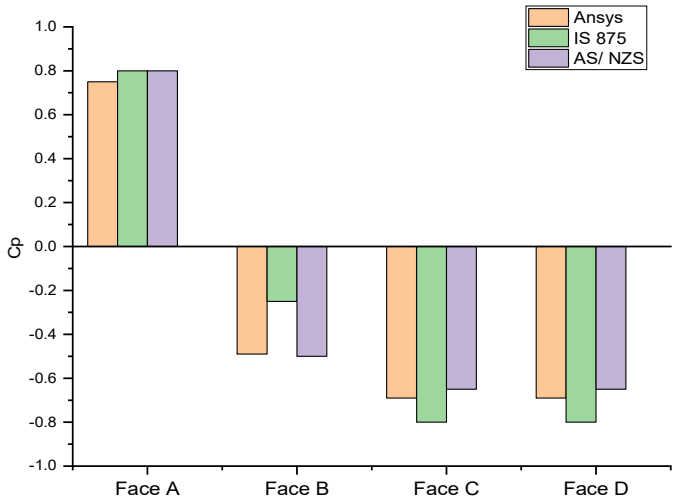

Figure 5-33 Comparison of mean pressure coefficients on a different face of all model for 0-degree between numerical result and International Standard

The face average Cp for different faces of different models for different angle of attack is summarized in table 5-2.

Table 5-2 Cp for different faces for different models at different angle of incidence

Building model	Angle of attack	Face A	Face B	Face C	Face D
Square	0°	+0.75	-0.49	-0.69	-0.69
	30°	+0.69	-0.53	-0.12	-0.66
	60°	-0.31	-0.58	+0.51	-0.55
	90°	-0.68	-0.65	+0.68	-0.45
Rectangle-1	0°	+0.74	-0.44	-0.66	-0.67
	30°	+0.69	-0.50	+0.14	-0.64
	60°	-0.30	-0.56	+.52	-0.53
	90°	-0.66	-0.62	+0.67	-0.43
Rectangle-2	0°	+0.74	-0.35	-0.62	-0.62
	30°	+0.68	-0.47	+0.15	-0.55
	60°	-0.30	-0.53	+.42	-0.49
	90°	-0.65	-0.61	+0.71	-0.36
Rectangle-3	0°	+0.73	-0.24	-0.59	-0.59
	30°	+0.67	-0.44	+0.17	-0.52
	60°	-0.29	-0.51	+0.57	-0.41
	90°	-0.61	-0.58	+0.74	-0.21

6 CONCLUSION

The pressure contour and mean pressure coefficients for the rectangular-shape building models for different side ratios at 0^0 ,30^0 ,60^0 and 90^0 wind incidence angles are compared in this paper. The *k*-ε model is used to simulate the results.

The major finding of this research are as follows:

- The influence of side ratios and wind orientations on wind pressure distribution and magnitude of pressure coefficients on rectangular building models is identified by numerical study measurement of wind pressures on building models.
- The variation of pressure coefficients on the centreline is discussed and shown graphically.
- Model side ratio has a significant impact on the amplitude and distribution of wind pressure on leeward and sidewalls, but only a little impact on windward walls when the wind incidence angle is zero.
- Changes in side ratio have little effect on the general magnitude of peak pressures and peak suctions in models with constant cross section.
- Comparison is made for numerical simulation data with various codes.

7 References

1) Nagar, S., & Ritu Raj. (2020). Experimental study of wind-induced pressures on tall buildings of different shapes. *Wind and Structures, Vol. 31, No. 5 (2020) 441-453*.
2) Ahuja, J. A. (n.d.). Effects of Side Ratio on Wind-Induced Pressure Distribution on Rectangular Buildings.
3) bailey, k. a. (1987-88). Effects of Aerodynamic Modifications of Building Shapes on Wind Induced Response of Tall Buildings.
4) Bairagi, A. M. (n.d.). Wind pressure and velocity pattern around 'N' plan shape tall building.
5) Dalui1, N. A. (n.d.). Aerodynamic analysis of pentagon-shaped tall buildings.
6) Dalui2, B. B. (n.d.). Experimental and Numerical Study of Wind-Pressure Distribution on Irregular-Plan-Shaped Building.
7) Dalui2, P. S. (n.d.). Comparison of aerodynamic coefficients of various types of Y-plan-shaped tall buildings.
8) Franke, J., & Hirsch, C. (n.d.). Recommendations on the use of CFD in wind engineering.
9) Kastner, P., & Dogan, T. (2020). Streamlining meshing methodologies for annual urban CFD simulations. *Journal of Energy and Buildings*.
10) M. Mallick, A. M. (n.d.). Modelling of Wind Pressure Coefficients on C-Shaped Building Models.
11) On the domain size for the steady-state CFD modelling of a tall building . (n.d.).
12) Pal, S., & Ritu Raj. (2021). Comparative study of wind induced mutual interference effects on square and fish-plan shape tall buildings. *Elsivier*.
13) Q.S. Li, J.Y. Fu, & Y.Q. Xiao. (n.d.). Wind tunnel and full-scale study of wind effects on China's tallest building.
14) R. Sheng a, b. L. (n.d.). Wind tunnel study of wind effects on a high-rise building at a scale of 1:300.
15) R. Sheng, L. Perret, & I. Calmet. (n.d.). Wind tunnel study of wind effects on a high-rise building at a scale of 1:300.
16) Suresh K Nagar1a, R. R. (n.d.). Experimental study of wind-induced pressures on tall buildings of different shapes.

17) R. Ahlawat and A. Ahuja, “Wind Loads on T Shape Tall Buildings,” *J. Acad. Ind. Res.*, vol. 24, no. 1, p. 257922, 2015.
18) R. Ahlawat and A. K. Ahuja, “Wind loads on Y plan shape tall building,” *Int. J. Eng. Appl. Sci.*, vol. 2, no. 4, p. 257946, 2015.
19) IS: 875 (2015), *Indian Standard design loads (other than earthquake) for buildings and structures-code of practice,part 3(wind loads)*. 2015.
20) ASCE: 7-10(2013), *Minimum Design Loads for Buildings and Other Structures. Structural Engineering Institute of the American Society of Civil Engineering, Reston*. 2013.
21) GB 50009-2001, *NATIONAL STANDARD OF THE PEOPLE’S REPUBLIC OF CHINA*. 2002.
22) AS/NZS:1170.2(2011), *Structural Design Actions - Part 2: Wind actions. Standards Australia/Standards New Zealand, Sydney*. 2011.
23) Hong Kong Building Department, “Code of Practice on Wind Effects in Hong Kong 2019,” 2019.